

Western  Graduate&PostdoctoralStudies

Western University
Scholarship@Western

Electronic Thesis and Dissertation Repository

4-23-2018 11:30 AM

Properties and Computation of the Inverse of the Gamma function

Folitse Komla Amenyoun
The University of Western Ontario

Supervisor
Jeffrey,David
The University of Western Ontario

Graduate Program in Applied Mathematics
A thesis submitted in partial fulfillment of the requirements for the degree in Master of Science
© Folitse Komla Amenyoun 2018

Follow this and additional works at: <https://ir.lib.uwo.ca/etd>



Part of the [Numerical Analysis and Computation Commons](#)

Recommended Citation

Amenyoun, Folitse Komla, "Properties and Computation of the Inverse of the Gamma function" (2018).
Electronic Thesis and Dissertation Repository. 5365.
<https://ir.lib.uwo.ca/etd/5365>

This Dissertation/Thesis is brought to you for free and open access by Scholarship@Western. It has been accepted for inclusion in Electronic Thesis and Dissertation Repository by an authorized administrator of Scholarship@Western. For more information, please contact wlsadmin@uwo.ca.

Abstract

We explore the approximation formulas for the inverse function of Γ . The inverse function of Γ is a multivalued function and must be computed branch by branch. We compare three approximations for the principal branch $\check{\Gamma}_0$. Plots and numerical values show that the choice of the approximation depends on the domain of the arguments, specially for small arguments. We also investigate some iterative schemes and find that the Inverse Quadratic Interpolation scheme is better than Newton's scheme for improving the initial approximation. We introduce the contours technique for extending a real-valued function into the complex plane using two examples from the elementary functions: the log and the arcsin functions. We show that, using the contours technique, the principal branch $\check{\Gamma}_0(x)$ has the extension $\check{\Gamma}_0(z)$ to the branch cut $\mathbb{C} \setminus]-\infty, \Gamma(\psi_0)]$ and the branch $\check{\Gamma}_{-1}(x)$ has the extension $\check{\Gamma}_{-1}(z)$ to the branch cut $\mathbb{C} \setminus]0, \Gamma(\psi_0)]$, where ψ_0 is the positive zero of $\Gamma'(x)$.

Keywords: Gamma function, inverse function, branch points, branch cut, extension, contours, Stirling formula, Ramanujan formula, Lambert function

Acknowledgements

I would to extend my gratitude to my supervisor Prof. David Jeffrey and Prof. Rob Corless for their support and guidance. I also want to thank Eunice Chan and Leili Rafiee Sevyeri at ORCA laboratory for their support. Lastly, thanks to everyone in the Department of Applied Mathematics at Western University.

Contents

Abstract	i
Acknowledgements	ii
List of Figures	vi
List of Tables	ix
1 Fundamental Properties of the Γ function	1
1.1 Introduction	1
1.2 Functional properties of the Γ function	3
1.2.1 Notation	3
1.2.2 Real-valued of Γ function	3
1.2.3 Complex-valued Γ	5
1.2.4 The log Γ function	5
1.3 Numerical approximations of the Γ function	9
1.3.1 Stirling formula	9
1.3.2 Lanczos approximation	13
1.3.3 Spouge approximation	14
1.3.4 Other approximations of Γ	14
1.4 Approximations for negative arguments	15
1.5 Approximations for complex arguments	16
1.6 Conclusion	16

2	Real Inverse function of Γ	17
2.1	Introduction	17
2.2	Notation and branches definition	17
2.3	Visualization of the Inverse function of Γ	19
2.4	The condition number of the Inverse function	20
2.5	Estimates for the principal branch $\check{\Gamma}_0$	22
2.5.1	Stirling-based approximation	23
2.5.2	Ramanujan-based approximation	25
2.6	Iterative Schemes	26
2.6.1	Newton Schemes	27
2.6.2	Inverse Quadratic Interpolation	29
2.6.3	Improving the estimates for small arguments	30
2.6.4	The rate of convergence near the turning point γ_0	32
2.7	Estimates for the branch $\check{\Gamma}_{-1}$	33
2.8	Estimates for other branches $\check{\Gamma}_k$	35
2.9	Conclusion	35
3	Complex Inverse function of Γ	37
3.1	Introduction	37
3.2	Notation	37
3.3	The extension of $\check{\Gamma}_k(x)$ to the complex plane	38
3.3.1	The extension of the log function in the complex plane	38
3.3.2	The extension of the arcsin function in the complex plane	41
3.3.3	The extension of the $\check{\Gamma}_0$ in the complex plane	43
3.3.4	The extension of the other branches $\check{\Gamma}_k$ in complex plane	47
3.4	Conclusion	49
	Bibliography	52

List of Figures

1.1	Real-valued plot of Γ . The dot points denote the extrema of Γ	4
1.2	Modulus plot of $\Gamma(z)$	6
1.3	A phase plot of $\Gamma(z)$. The colours represent the points that have the same argument	7
1.4	(a) $d\Gamma/dx$. (b) $d^2\Gamma/dx^2$	7
1.5	(a) $d \log \Gamma/dx$. (b) $d^2 \log \Gamma/dx^2$	8
1.6	$\Gamma(x)$ and others asymptotic approximations	11
1.7	$\Gamma(x)$ and other approximations for small values	12
1.8	$\Gamma(x)$ and other approximations for small values	12
1.9	The condition number Eq. (1.20) of $\Gamma(x)$ and other approximation for small values.	13
1.10	$\Gamma(x)$ and approximation (1.29). The red dashed lines are the approximation, and the blue dotted lines show $\Gamma(x)$	15
1.11	A comparison of the Gamma function and Stirling's formula in the complex plane.	16
2.1	(a) Real-valued Γ . (b) Real-valued Inverse of Γ . Note the poles in Γ at non-positive integers become the critical points in $\check{\Gamma}$ where the branch changes. The ranges of the branches are shown labelled with k	19
2.2	The principal branch $\check{\Gamma}_0$ (red) compared to the \ln function (blue). The \ln function grows faster than the principal branch. Note that the \log function is placed below the principal branch, but will eventually overtake the Inverse Gamma function.	20

2.3	The condition number of the inverse function of Γ . Eq. (2.10)	22
2.4	(a) $\check{\Gamma}_0(x)$ (red solid) and the approximation (2.12)(blue solid) for larger argument range.(b) For small argument range.	23
2.5	(a) $\check{\Gamma}_0(x)$ (red solid) and the approximation (2.13) (blue) .(b) For small argument range	24
2.6	(a) $\check{\Gamma}_0(x)$ (red solid) the approximation (2.25)(blue solid).(b) For small argument range.	27
2.7	(a) Estimates around the turning point γ_0 for approximation (2.26),(b) Estimates around the turning point γ_0 for approximation (2.31)	31
2.8	$\check{\Gamma}_{-1}(x)$ (solid red), the approximation 2.33(blue solid) and 2.34(solid green)	34
2.9	(a) The branch $\check{\Gamma}_{-2}(x)$. The branch $\check{\Gamma}_{-3}(x)$	35
3.1	Domain and range for complex function mapping in the complex plane .	39
3.2	Extending the $\log(x)$ function into the complex plane. The straight contours are trimmed in w -range so that their images do not collide in the z -domain	40
3.3	Extending the $\log(x)$ function into the complex plane. The straight contours are trimmed in w -range so that their images do not collide in z -domain. Adding the slight slope to the lines makes the collision easier to see.	40
3.4	The range of the Principal value $\log z$ in the complex plane.	41
3.5	The range of the branch $k = 1$ of $\log(z)$ in the complex plane, denoted $\ln_1 z$.	42
3.6	Extending the $\arcsin(x)$ function into the complex plane. The straight contours do not need to be trimmed in w -range, and yet the images show the branch cuts clearly.	42
3.7	Extending the $\arcsin(x)$ function into the complex plane. The straight contours above the real axis in the z -domain have been slightly offset relative to those below the axis, so that the collisions are easily seen. . .	43
3.8	Extending the Principal branch of the inverse of $\Gamma(z)$ into the complex plane	43

3.9	Zoom of 3.8(a)	44
3.10	The range of the Principal branch of the Inverse function of $\Gamma(z)$ in the complex plane	45
3.11	Extending the Principal branch of the inverse of $\Gamma(z)$ into the complex plane. Contours not starting from the real axis.	47
3.12	The range of the principal branch. The dotted line shows an approximation to the boundary. The large dots are points on the boundary showing how it extends for values with negative real part.	47
3.13	The extension of the positive $\check{\Gamma}_{-1}(x)$ into the complex plane	48
3.14	The extension of the negative $\check{\Gamma}_{-1}(x)$ into the complex plane	48
3.15	The extension of the positive $\check{\Gamma}_{-1}(x)$ into the complex plane	49
3.16	The range of the branch $\check{\Gamma}_{-1}$ in the complex plane.	50
3.17	A schematic presentation of the ranges of the branches of $\check{\Gamma}_k$ in the complex plane, for $k \leq 0$.	51

List of Tables

1.1	10 extrema points of Γ	4
2.1	Critical values or turning points for branches of $\check{\Gamma}_k$	18
2.2	Branches of $\check{\Gamma}_k$ and their range	18
2.3	Numerical values of $\check{\Gamma}_0(x)$, approximation (2.12) and (2.13)	24
2.4	Error for solving $\Gamma(y) - 0.93$ for y given an initial y_0	28
2.5	Error for solving of $\Gamma(y) - 1$ for y given an initial y_0	29
2.6	Newton and Inverse Quadratic Interpolation for solving $\Gamma(y) - 0.93$ for y	30
2.7	Numerical values of approximation (2.12) and approximation (2.13) . . .	32
2.8	Number of iterations near $x = \gamma_0$ for branch $k = 0$. The starting estimate was based on Eqn (2.31). The columns correspond to Newton's method (NM) and our quadratic scheme (QS). The iteration was continued until the relative error was less than 10^{-16}	33
2.9	Numerical values of the approximation (2.12), (2.34) and (2.35)	34
3.1	Numerical computation of $\check{\Gamma}_0$ for larger arguments	45

Chapter 1

Fundamental Properties of the Γ function

1.1 Introduction

The Γ function¹ is one of the most important special functions in mathematics and has numerous applications, including combinatorics, statistics, probability theory, quantum mechanics, and solid-state physics. The Gamma function is defined in different ways in the literature; there are equivalences between the definitions, and some of the equivalences are trivial to prove, while others need more elaboration. We shall introduce a few fundamental definitions of the Γ function and refer the reader to the literature for other definitions and proofs. The first definition of Γ started from the idea of extending the positive integer factorial $n = n(n - 1)(n - 2) \dots 2 \cdot 1$ to real numbers. The Γ function is an extension of the factorial function with an argument shifted by 1, to real numbers and complex numbers.

$$\Gamma(z) = (z - 1)! = \int_0^{\infty} t^{z-1} e^{-t} dt, \quad \Re(z) > 0. \quad (1.1)$$

¹Some authors write “the Gamma function” and some just refer to it with the Greek letter Γ .

The above definition of Γ by an improper integral converges absolutely for $\Re(z) > 0$ and one can use integration by parts to show the recurrence or functional relation

$$\Gamma(z + 1) = z\Gamma(z) . \quad (1.2)$$

Inverting the relation, we have

$$\Gamma(z) = \frac{\Gamma(z + 1)}{z} . \quad (1.3)$$

The above equation is important as it's used to extend the $\Gamma(z)$ defined in (1.1) to a meromorphic and more general Γ function for all complex numbers, except the negative integers. The Γ function is singular at negative integers $z = -1, -2, \dots$ with simple poles and the residues at these points are

$$\text{Res}(\Gamma, -n) = \frac{(-1)^n}{n!} , \quad n \in \mathbb{N} . \quad (1.4)$$

Another definition of the Γ function is sometimes called the Weierstrass form and defined by

$$\frac{1}{\Gamma(z)} = ze^{\gamma z} \prod_{k \geq 1} \left(1 + \frac{z}{k}\right) e^{-z/k} , \quad z \in \mathbb{C} \setminus \{-1, -2, -3, \dots\} , \quad (1.5)$$

where $\gamma \approx 0.577721 \dots$ is called the Euler-Mascheroni constant.

Another property of the Γ function is the reflection formula

$$\Gamma(1 - z)\Gamma(z) = \frac{\pi}{\sin \pi z} , \quad z \notin \mathbb{Z} . \quad (1.6)$$

The Γ function does not have a closed form and must be approximated. For generations, many researchers, including mathematicians, physicists, numbers theorists and statisticians, have proposed numerous approximations for the computation of the Γ function. The rest of this chapter will be devoted to the review of some of the most recent numerical approximations of Γ . First, we shall, in the following paragraphs, remind the reader

of some of the most fundamental functional properties of the function that make it a very special function. For a full review of the properties of Γ and related functions, see [1].

1.2 Functional properties of the Γ function

1.2.1 Notation

Most books and references adopted the convention of writing $\Gamma(x)$ when referring to real-valued Γ and $\Gamma(z)$ when referring to the complex-valued Γ . We will adopt the same convention in this thesis.

1.2.2 Real-valued of Γ function

Figure 1.1 shows the real-valued plot of $\Gamma(x)$. Poles occur at negative integers. The dots points are the extrema of Γ . The derivation $\Gamma'(x)$ can be defined in terms of the logarithm derivation or digamma or psi function.

$$\Psi(x) = \frac{d}{dx} \ln \Gamma(x) . \quad (1.7)$$

The n -order logarithmic derivation, also called the polygamma function is defined as

$$\Psi(n, x) = \frac{d^n}{dx^n} \ln \Gamma(x) . \quad (1.8)$$

Table 1.1 shows the 10 extrema of the Γ function and the values Γ at these points. A few particular values of the Γ function can be computed using the reflection formula

$$\Gamma\left(\frac{1}{2}\right) = \sqrt{\pi}$$

by replacing z by $1/2$ in the reflection

$$\Gamma(0) = 0! = 1$$

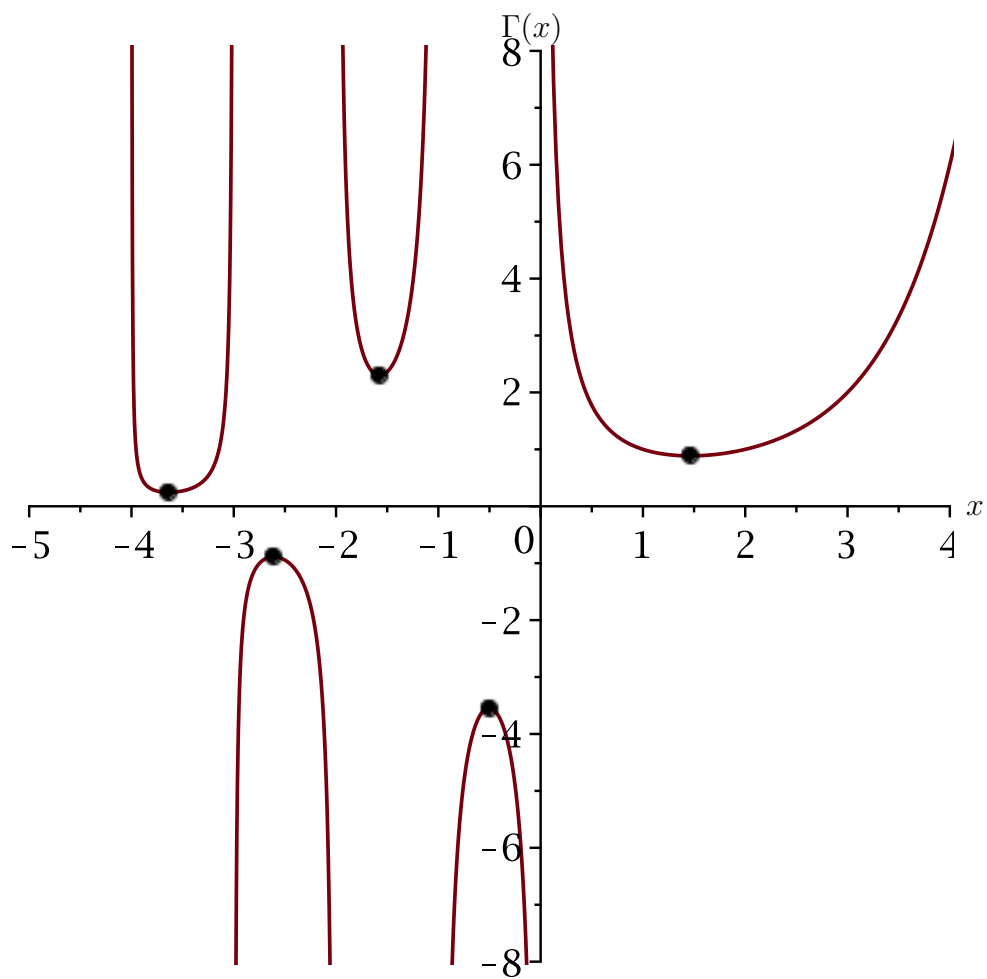


Figure 1.1: Real-valued plot of Γ . The dot points denote the extrema of Γ

x	$\Gamma(x)$
1.46163	0.885603
-0.50408	-3.544644
-1.57349	2.302407
-2.61072	-0.888136
-3.63529	0.245127
-4.65323	-0.052780
-5.66716	0.009324
-6.67841	-0.001397
-7.68778	0.000181
-8.68576	-0.000020

Table 1.1: 10 extrema points of Γ

$$\Gamma\left(-\frac{1}{2}\right) = -2\sqrt{\pi}$$

Using the reflection formula $\Gamma\left(\frac{3}{2}\right)\Gamma\left(-\frac{1}{2}\right) = -\sqrt{\pi}$ and the recurrence relation $\Gamma(z + 1) = z\Gamma(z)$

1.2.3 Complex-valued Γ

The graph of a complex function in one variable produces a surface in 4-dimensional space and this is difficult to picture in our minds because we can only picture 3-D objects. The development of mathematical tools and software environments in recent years has encouraged many visualization techniques, see [25]. But the plot of the modulus, also called analytical plot, and the portrait phase plot still remain the technique widely used for the visualization of complex-valued functions. Figure 1.2 and 1.3 show respectively the modulus and the phase plot of $\Gamma(z)$. On figure 1.3, the colours represent the points that have the same argument.

1.2.4 The log Γ function

The monotonicity and the convexity of the Γ and functions related to the Γ has attracted the attention of many authors and are discussed in many papers, see [9, 2, 4]. And it is known that the Γ function is convex only for positive real arguments and is logarithmically convex on the whole \mathbb{R} domain. A practical way to verify this is to use the fact that:

- The derivative of a convex function g of one real variable on the interval $[\alpha, \beta] \subseteq \mathbb{R}$ is monotonically increasing
- The second-derivative of a convex function g of one real variable on the interval $[\alpha, \beta] \subseteq \mathbb{R}$ is positive $\forall x_1, x_2 \in [\alpha, \beta]$.

For Γ function, the derivative is given by

$$\frac{d}{dx}\Gamma(x) = \Psi(x)\Gamma(x) \tag{1.9}$$

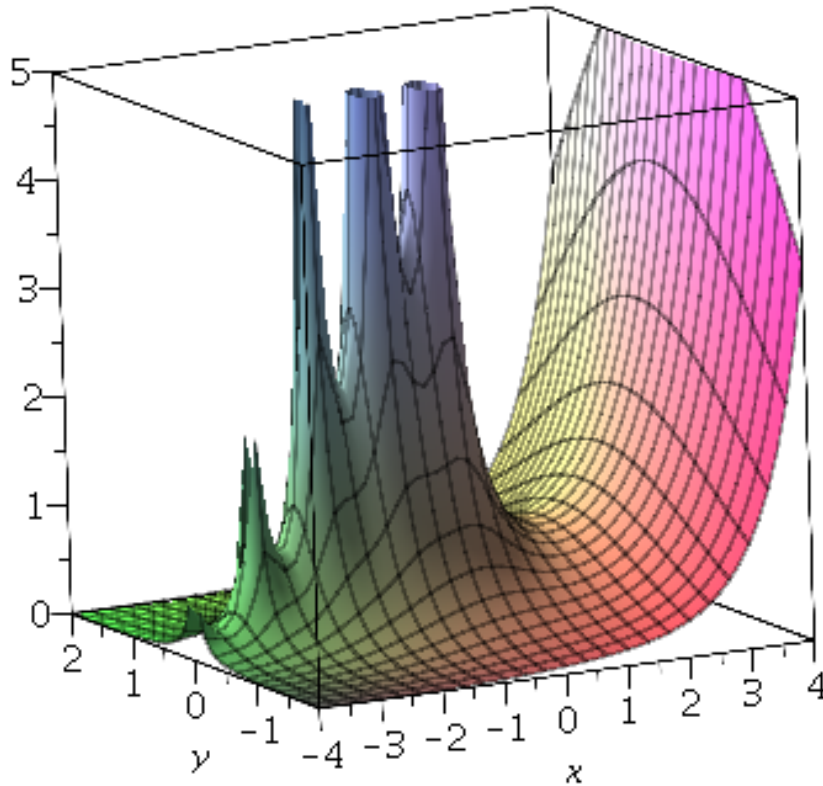


Figure 1.2: Modulus plot of $\Gamma(z)$.

and the second derivative is given by

$$\frac{d^2}{dx^2}\Gamma(x) = \Psi(1, x)\Gamma(x) + \Psi(x)^2\Gamma(x) \quad (1.10)$$

Figure 1.4 plots the derivative and second derivative of the real-valued Γ . The graph of $d\Gamma/dx$ is not that much informative but the graph $d^2\Gamma/dx^2$ clearly shows $d^2\Gamma/dx^2 > 0 \forall x \in \mathbb{R}_+$.

For the log-convex property of the Γ function, we use the Weierstrass form

$$\frac{1}{\Gamma(x)} = xe^{\gamma x} \prod_{n=1}^{\infty} \left(1 + \frac{x}{n}\right) e^{-x/n} \quad (1.11)$$

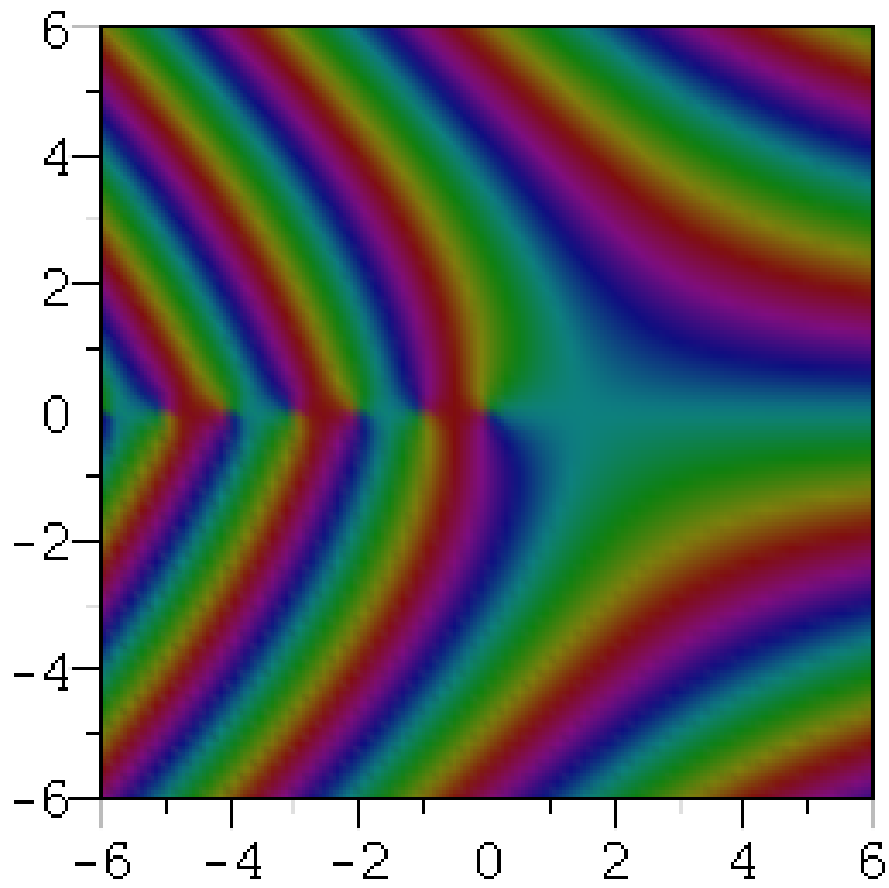


Figure 1.3: A phase plot of $\Gamma(z)$. The colours represent the points that have the same argument

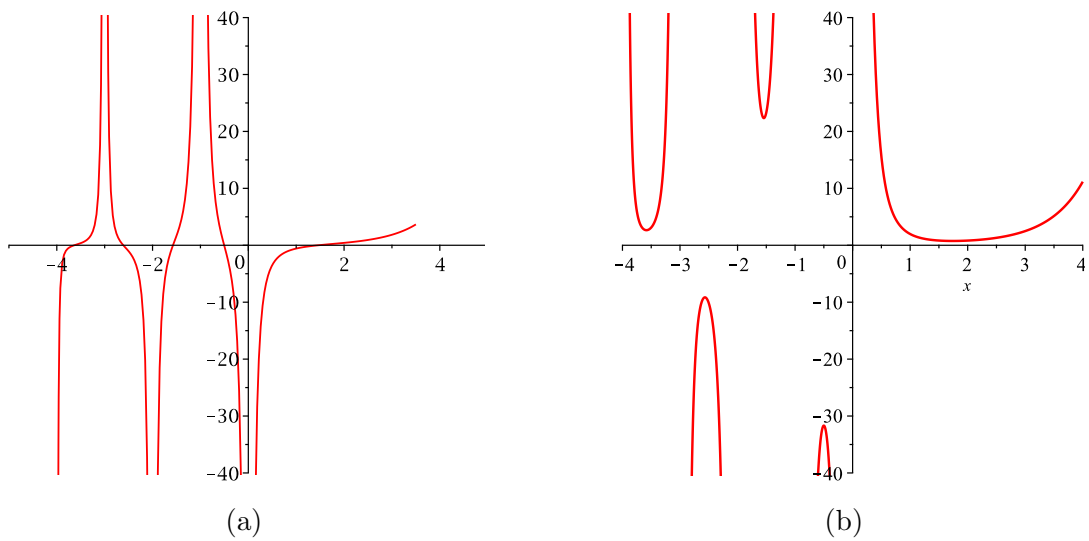


Figure 1.4: (a) $d\Gamma/dx$. (b) $d^2\Gamma/dx^2$

$$\log \Gamma(x) = -\log x - \gamma x + \sum_{n=1}^{\infty} \left(\frac{x}{n} - \log\left(1 + \frac{x}{n}\right) \right) \quad (1.12)$$

The derivative of $\log \Gamma(x)$ is exactly what is called the digamma function

$$\frac{d}{dx}(\log \Gamma(x)) = \Psi(x) = \frac{\Gamma'(x)}{\Gamma(x)} = -\gamma + \sum_{n=0}^{\infty} \left(\frac{1}{n+1} - \frac{1}{x+n} \right) \quad (1.13)$$

and the second derivative of the $\log \Gamma(x)$ is

$$\frac{d^2}{dx^2}(\log \Gamma(x)) = \Psi(1, x) = \sum_{n=0}^{\infty} \frac{1}{(x+n)^2} \quad (1.14)$$

Figure 1.5 (a) shows the plot of the $d(\log \Gamma)/dx$. It has vertical asymptotes at the points $-n$. On each interval $(-n, -n+1)$, $n \geq 1$, the function Ψ increases strictly. Figure 1.5 (a) also shows the unique points $x_n \in (-n, -n+1)$, $n \geq 1$, such that $\Psi(x_n) = 0$ or equivalently $\Gamma'(x_n) = 0$. Also, figure 1.5 (b) shows $d^2 \log \Gamma/dx^2 > 0, \forall x \in \mathbb{R}$

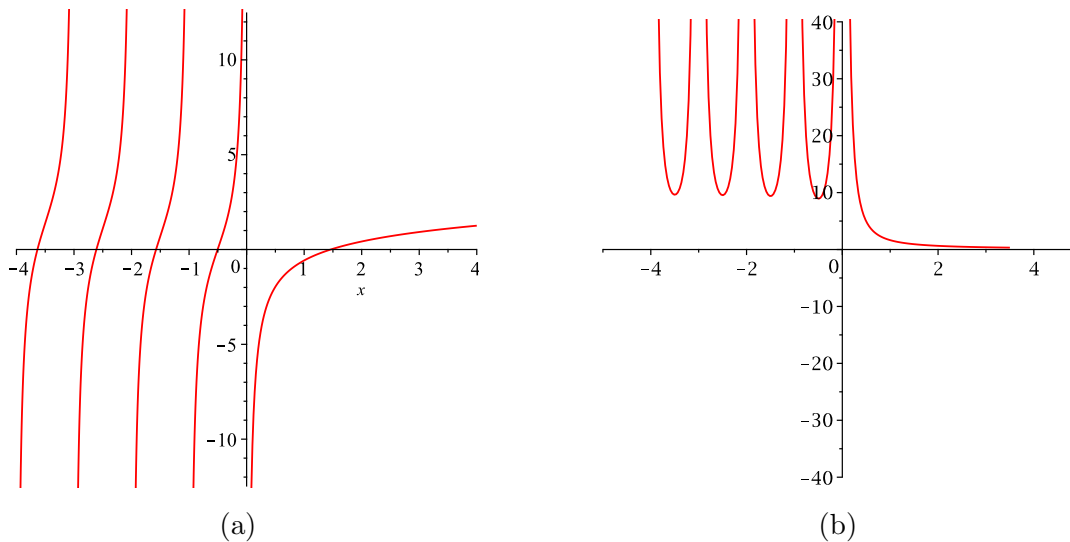


Figure 1.5: (a) $d \log \Gamma/dx$. (b) $d^2 \log \Gamma/dx^2$

1.3 Numerical approximations of the Γ function

The numerical computation of the Γ function has attracted the attention of many researchers for generations, all trying to establish the approximation formula that best computes the Γ function. Many approximation methods have been proposed so far in the scientific literature. See, [12, 22, 21, 6, 17, 18]. Software libraries and computing environments use combinations of these approximations formulas to implement their routines for Γ . In the following sections, we give a brief overview of the approximations of the Γ function. Most approximations treat the real-valued Γ .

1.3.1 Stirling formula

The Stirling approximation is, so far, the most well-known and most-cited approximation for the Γ function and it is defined as

$$\begin{aligned} \Gamma(x+1) &\sim \sqrt{2\pi x} \left(\frac{x}{e}\right)^x \exp\left(\sum_{m=1}^{\infty} \frac{B_{2m}}{2m(2m-1)x^{2m-1}}\right) \\ &= \sqrt{2\pi x} \left(\frac{x}{e}\right)^x \exp\left[\frac{1}{12x} - \frac{1}{360x^3} + \frac{1}{1260x^5} - \frac{1}{1680x^7} + \dots\right], \quad x \rightarrow \infty \end{aligned} \tag{1.15}$$

where the B_n are the Bernoulli numbers.

Other formulas that are related to the Stirling formula are the Laplace formula, see [24]

$$\Gamma(x+1) \sim \sqrt{2\pi x} \left(\frac{x}{e}\right)^x \left[1 + \frac{1}{12x} + \frac{1}{288x^2} - \frac{139}{51840x^3} - \frac{571}{2488320x^4} + \dots\right], \quad x \rightarrow \infty \tag{1.16}$$

and the Ramanujan formula, see [24]

$$\Gamma(x+1) \sim \sqrt{2\pi x} \left(\frac{x}{e}\right)^x \left[1 + \frac{1}{2x} + \frac{1}{8x^2} + \frac{1}{240x^3} - \frac{11}{1920x^4} + \frac{79}{26880x^5} \dots\right]^{1/6}, \quad x \rightarrow \infty \tag{1.17}$$

In [17], the author finds an explicit formula for the computation of the coefficients of the expansion in the series of the expression

$$\exp\left(\sum_{m=1}^{\infty} \frac{B_{2m}}{2m(2m-1)x^{2m-1}}\right) \quad (1.18)$$

and gives the following asymptotic approximation

$$\Gamma(x+1) \sim \sqrt{2\pi x} \left(\frac{x}{e}\right)^x \left[1 + \frac{1}{12x^2} + \frac{1}{1440x^3} + \frac{239}{36288x^6} + \dots\right]^x, \quad x \rightarrow \infty \quad (1.19)$$

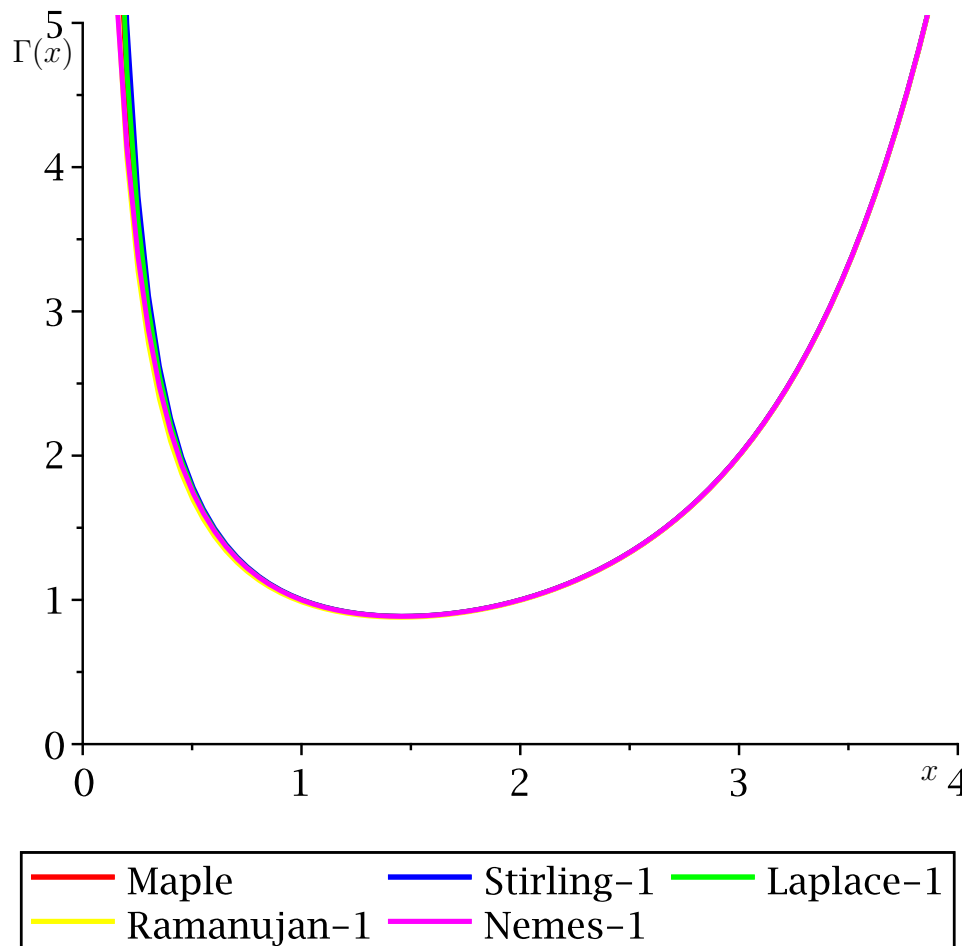
We compare the four approximations mentioned above with the Γ routine implemented in Maple. Maple guarantees that every built-in function will return numerical values accurate to 0.6ULP² at the current setting of the environmental variable `Digits`; ULP means Units in the Last Place. In what follows we shall assume that Maple's approximation satisfies their promise.

Figure 1.6 shows Maple's values and the four approximation formulas, where the number that follows the name of the approximation is the exponent of $(1/x)$ of the last term kept in the series expansion. As expected, the graphs of the approximations overlap for larger values of the argument x because they are all asymptotic approximations. It is almost impossible to see the different colours used to depict the graph of each approximation.

For small values of x , the difference between the approximations starts to appear and if we zoom the figure 1.6 in the range $x \in [0, 0.5]$, we get figure 1.7 and figure 1.8.

Figure 1.7 (a) shows that Laplace-1 gives a better approximation than Ramanujan-1 and Nemes-2, however figure 1.7 (b) and figure 1.8 (a) show that Ramanujan-2 and Ramanujan-3 outperform the corresponding Laplace-2 and Laplace-3, and Nemes-4. In all cases, Ramanujan approximation seems to be the approximation that closely agrees with the Maple Γ built-in function for small values. Another interesting remark is that the slope of the graph of Nemes and Ramanujan approximations have almost no change

²ULP is discussed in chapter 3 of [5]

Figure 1.6: $\Gamma(x)$ and others asymptotic approximations

as more terms are added in the series expansion. Numerically, it suggests these approximations are more stable than Laplace's and Stirling's. We assess the stability of the approximations by computing and plotting their condition numbers. For the evaluation of a function $y = f(x)$, the condition number is given in [5]

$$C(x) = \frac{x f'(x)}{f(x)} \quad (1.20)$$

Figure 1.9 plots the condition number of the five approximations and we can see that Maple, Ramanujan and Nemes approximations are well conditioned for small values of x as the condition is constant $C(x) \rightarrow -1$ as $x \rightarrow 0$. Note that the condition number of

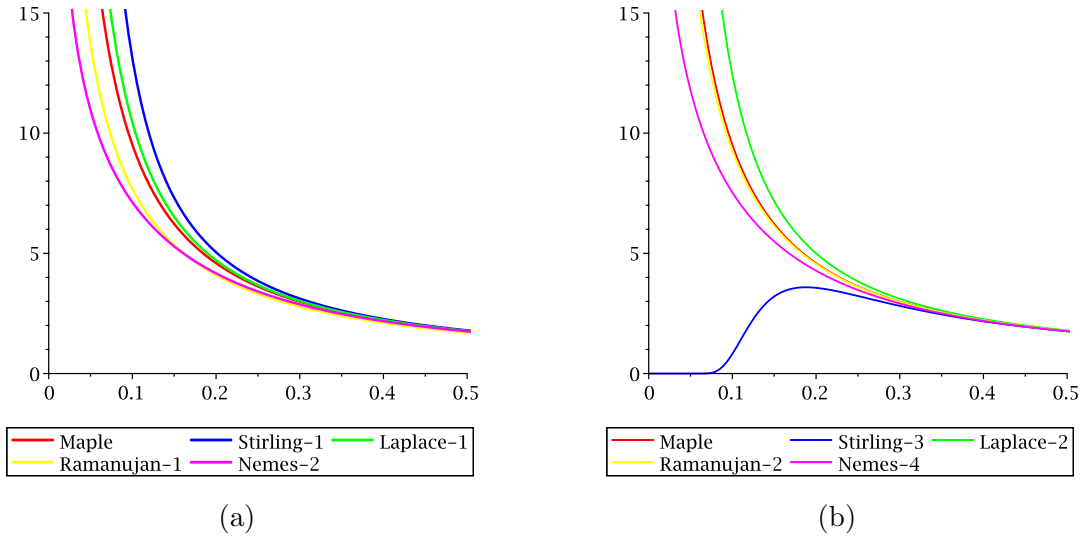


Figure 1.7: $\Gamma(x)$ and other approximations for small values

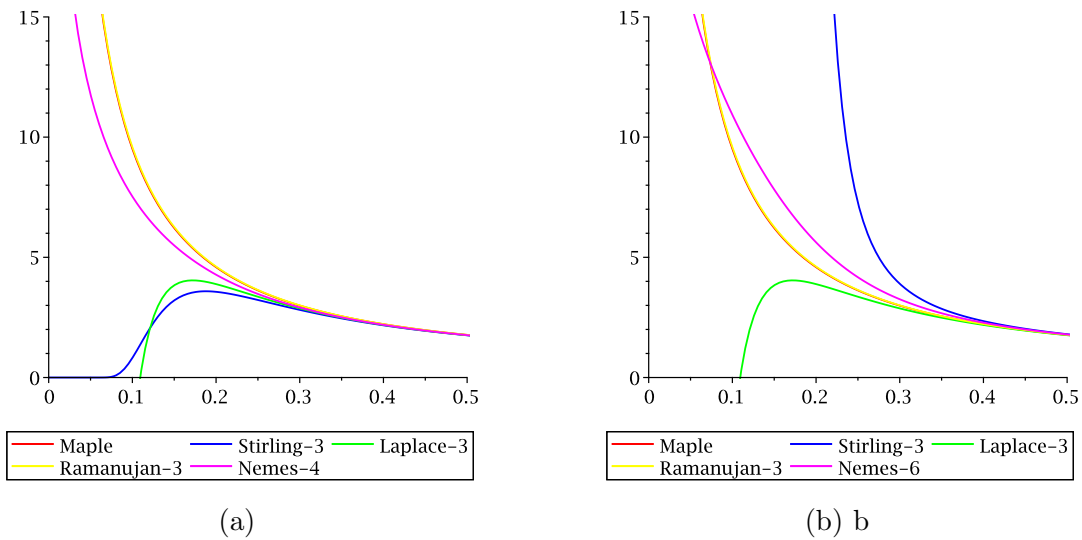


Figure 1.8: $\Gamma(x)$ and other approximations for small values

Ramanujan approximation is shadowed by the red colour of the Maple approximations suggesting that the Maple routine is based on the Ramanujan approximation. The Stirling and Laplace approximations are poorly conditioned for small values of x and their condition number values change sporadically and becomes huge.

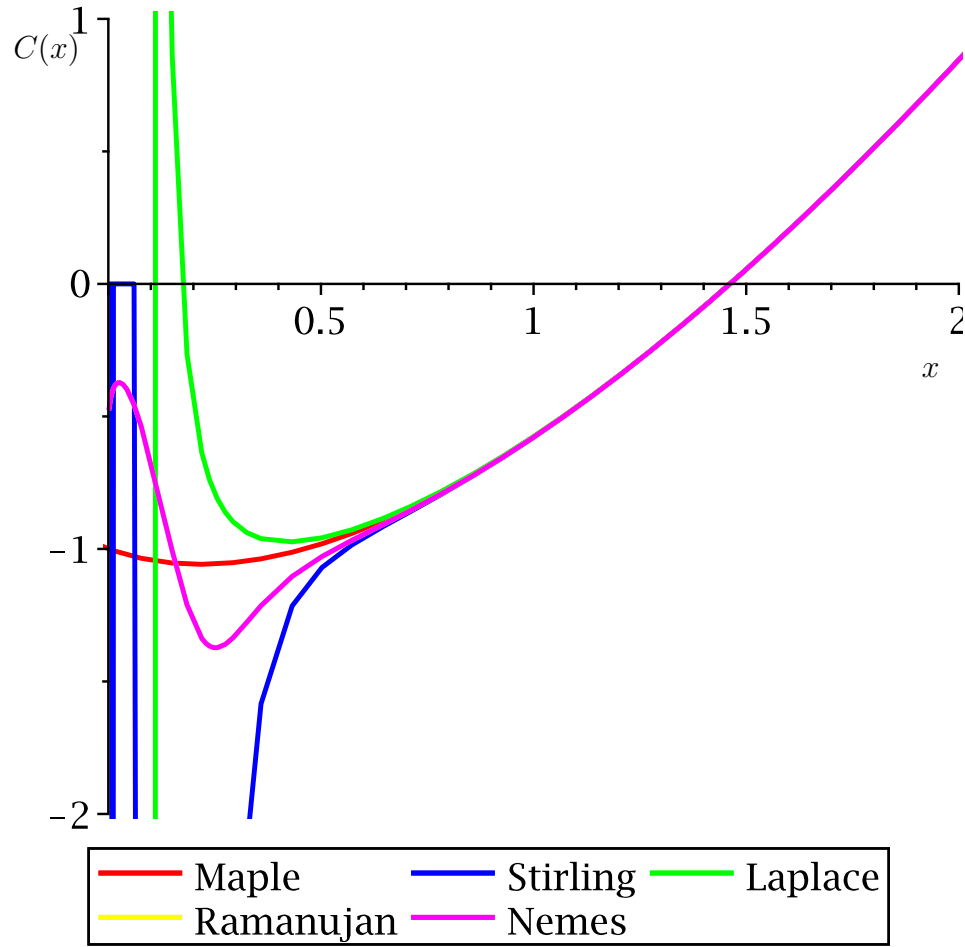


Figure 1.9: The condition number Eq. (1.20) of $\Gamma(x)$ and other approximation for small values.

1.3.2 Lanczos approximation

Another well-known and well-cited approximation of the Γ function is the Lanczos approximation introduced in 1964 in the paper [12] defined as

$$\Gamma(x+1) \approx \sqrt{2\pi} \left(z+r+\frac{1}{2}\right)^{z+1/2} e^{-(z+r+1/2)} S_r(z) \quad (1.21)$$

where

$$S_r(z) = \frac{1}{2}a_0(r) + a_1(r)\frac{z}{z+1} + a_2(r)\frac{z(z-1)}{(z+1)(z+2)} + \dots \quad (1.22)$$

A comprehensive study of the Lanczos approximation can be found in [20].

1.3.3 Spouge approximation

Another approximation of the Γ function is the Spouge formula [22]. It is defined by

$$\Gamma(x+1) \approx \sqrt{2\pi} e^{-(z+a)} (z+1)^{z+1/2} \left(c_0 + \sum_{k=0}^N \frac{C_k}{z+k} + \epsilon(z) \right) \quad (1.23)$$

where $\Re(z+a) > 0$ and $a \in \mathbb{R}$, $N = \lceil a \rceil - 1$, and $c_k(a)$ is defined by the recurrence

$$\begin{aligned} c_0(a) &= 1 \\ c_k(a) &= \frac{1}{\sqrt{2\pi}} \frac{(-1)^{k-1}}{(k-1)!} (-k+a)^{k-1/2} e^{-k+a} \end{aligned} \quad (1.24)$$

1.3.4 Other approximations of Γ

There are many approximations of the Γ function. A comprehensive list of these approximations can be found in [14]. Most of the approximations are asymptotic, meaning they accurately compute Γ function for large values of x in the real case and $|z|$ in the complex case. Also, most of the approximations have the similar algebraic form and can be described by more general formulas. This is the work of [16, 15] who introduced a couple of family of approximations.

$$\Gamma(x+1) \sim \sqrt{2\pi e} e^{-a} \left(\frac{x+a}{e} \right)^{x+\frac{1}{2}}, \quad x \rightarrow \infty \quad (1.25)$$

where $a \in \mathbb{R}$ and $a \in [0, 1]$. Recently, [24] proposed two general approximations and showed that other approximations are just special cases of his proposed approximation.

$$\Gamma(x+1) \sim \sqrt{2\pi x} \left(\frac{x}{e} \right)^x \frac{1}{e^a} \left(1 + \frac{b}{x} \right)^{cx+d} \left(\sum_{n=0}^{\infty} \frac{\alpha_n}{(x+h)^n} \right)^{\frac{x}{r}+q}, \quad x \rightarrow \infty \quad (1.26)$$

$$\Gamma(x+1) \sim \sqrt{2\pi x} \left(\frac{x}{e} \right)^x \frac{1}{e^a} \left(1 + \frac{b}{x} \right)^{cx+d} \exp \left(\sum_{n=0}^{\infty} \frac{\psi_n}{(x+h)^n} \right), \quad x \rightarrow \infty \quad (1.27)$$

where the coefficients α_n and ψ_n are obtained by recurrences.

1.4 Approximations for negative arguments

Stirling's formula and related approximations apply to positive real arguments. Approximations for negative arguments are not usually considered, but can be constructed easily.

We rewrite the reflection formula (1.6) using $x = -X$, so that $X > 0$, as

$$\Gamma(x) = \Gamma(-X) = \frac{\pi}{\sin(-\pi X)\Gamma(1+X)}. \quad (1.28)$$

We now approximate $\Gamma(1+X)$ using Stirling's approximation (1.15) and obtain

$$\Gamma(x) \approx \frac{\pi}{\sin(-\pi X)\sqrt{2\pi X}X^Xe^{-X}} = \sqrt{\frac{\pi}{2}} \left(\frac{e}{X}\right)^X \frac{-1}{\sqrt{X}\sin(\pi X)}. \quad (1.29)$$

Plots of $\Gamma(x)$ and its approximation are shown in figure 1.10.

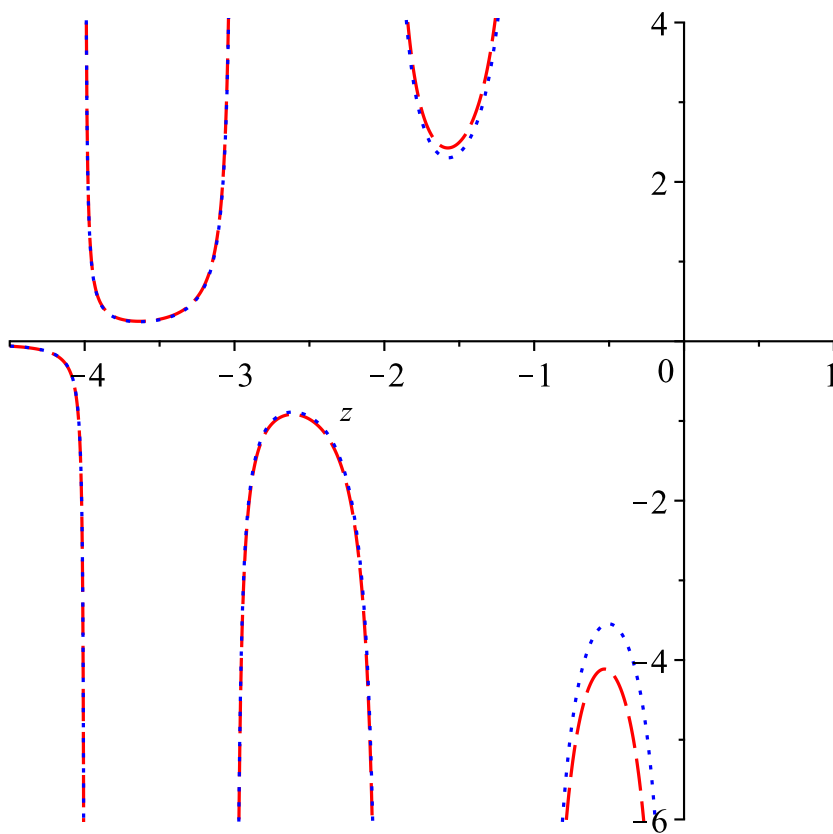


Figure 1.10: $\Gamma(x)$ and approximation (1.29). The red dashed lines are the approximation, and the blue dotted lines show $\Gamma(x)$.

1.5 Approximations for complex arguments

The many publications concerning Stirling's and similar formulas discuss only real positive arguments of the function. We have checked its validity in the complex plane as well. We compare the real and imaginary parts of $\Gamma(z)$ and Stirling's approximation on a contour parallel to the imaginary axis. Figure 1.11 plots $\Gamma(2 + iy)$ and the corresponding Stirling's formula for $|y| \leq 10$. Even so close to the imaginary axis, the approximation is very good. Further from the imaginary axis, the approximation is even better.

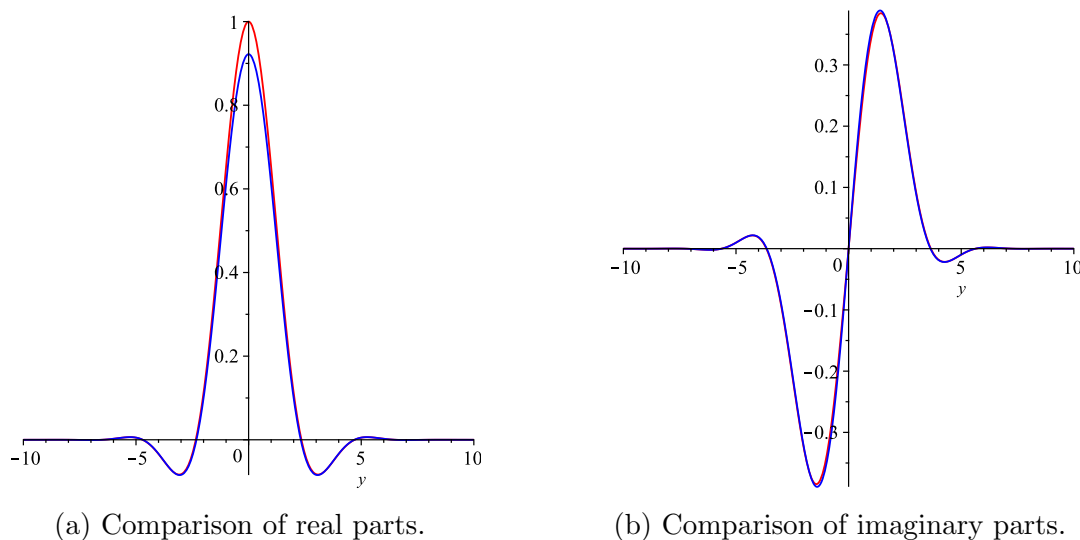


Figure 1.11: A comparison of the Gamma function and Stirling's formula in the complex plane.

1.6 Conclusion

In this chapter, we reviewed some of the fundamental properties of the Gamma function. We also covered some approximations of the Γ function. An important challenge that must be addressed, while suggesting an approximation formula for the Γ function is that the approximation method must be optimized for small values of the argument. In the next chapter, we shall use some of the approximation of the Γ for the computation of the Inverse function of Γ .

Chapter 2

Real Inverse function of Γ

2.1 Introduction

The Inverse function of Γ has applications in computer science [8]. It is a multivalued function. In a recent review of Γ in [1] the authors have pointed out that the Inverse function of Γ has received less attention. Some of the basic properties of the Inverse function of Γ were studied in [19]. In the papers [23] and [19], the authors showed that the Principal branch or the Principal Inverse of the Inverse function of Γ has an extension to a Pick function ¹ in the cut plane $\mathbb{C} \setminus]-\infty, \Gamma(\psi_0)]$, where $\psi_0 \approx 1.4616\dots$. But there is no study of the numerical and symbolic computation of the Inverse function of Γ . In this chapter and the next, we intend to explore some numerical procedures for the computation of the branches of the Inverse function of Γ .

2.2 Notation and branches definition

We denote the Inverse function of $\Gamma(x)$ by $w = \check{\Gamma}_k(x)$, where k labels the branch. The extrema of the Γ function defined by

$$\frac{d}{dx}\Gamma(x) = \Gamma(x)\Psi(x) = 0 \tag{2.1}$$

¹See reference [19] for the definition of Pick functions

and we denote these points (ψ_i, γ_i)

$$\begin{cases} \Psi(\psi_0) = 0 & \text{where } \psi_0 > 0 \\ \Psi(\psi_k) = 0 & \text{where } k < 0 \text{ and } k < \psi_k < k + 1 \end{cases}$$

Numerical values of these points are displayed in table 2.1. The branches $\check{\Gamma}_k$ are defined

k	ψ_k	$\gamma_k = \Gamma(\psi_0)$
0	1.461632	0.885603
-1	-0.504083	-3.544644
-2	-1.573498	2.302407
-3	-2.610720	-0.888136
-4	-3.635293	0.245127
-5	-4.653237	-0.052780

Table 2.1: Critical values or turning points for branches of $\check{\Gamma}_k$

by the interval or the domain of the arguments and the range of $\check{\Gamma}_k$ is displayed in table 2.2. Using the notation $x = \Gamma(y)$, and $y = \check{\Gamma}_k(x)$, if x falls outside the intervals shown above, $\check{\Gamma}$ becomes complex-valued. The numbering is chosen so that $k = 0$ corresponds

k	Arguments Intervals	Range of $\check{\Gamma}_k$
0	$x \geq \gamma_0$	$\psi_0 \leq \check{\Gamma}_0$
-1	$x > \gamma_0$ $x \leq \gamma_{-1}$	$0 < \check{\Gamma}_{-1} < \psi_0$ $\psi_{-1} \leq \check{\Gamma}_{-1} < 0$
-2	$x < \gamma_{-1}$ $x > \gamma_{-2}$	$-1 < \check{\Gamma}_{-2} < \psi_{-1}$ $\psi_{-2} \leq \check{\Gamma}_{-2} < -1$

Table 2.2: Branches of $\check{\Gamma}_k$ and their range

to the principal branch or principal Inverse and the remaining branches receive negative numbers so that the labels follow roughly the range taken by the branches. We notice some special values, since $\Gamma(2) = 1! = \Gamma(1) = 0! = 1$, the corresponding Inverse must lie on different branches. This requires $\check{\Gamma}_0(1) = 2$ and $\check{\Gamma}_{-1}(1) = 1$. Some other special values of interest are $\check{\Gamma}_0(\sqrt{\pi}/2) = 3/2$, which lies very close to the branch point and

$\check{\Gamma}_{-1}(\sqrt{\pi}) = 1/2$. In this chapter, we will denote the approximations of the Inverse function of Γ by $y(x)$, where x is the real argument.

2.3 Visualization of the Inverse function of Γ

We can plot the real-valued Inverse function of Γ using the known procedure for Γ . Recall that the plot command in Maple for $x = \Gamma(y)$, given an input y , is

```
plot([y,GAMMA(y),y = a..b],discont=true,view = [a..b,c..d])
```

The plot of the Inverse function of $\Gamma(y)$ is obtained by exchanging x and y , that is $y = \check{\Gamma}_k(x)$ and the Maple command becomes

```
plot([GAMMA(x),x,x=c..d],discont=true,view = [a..b,c..d])
```

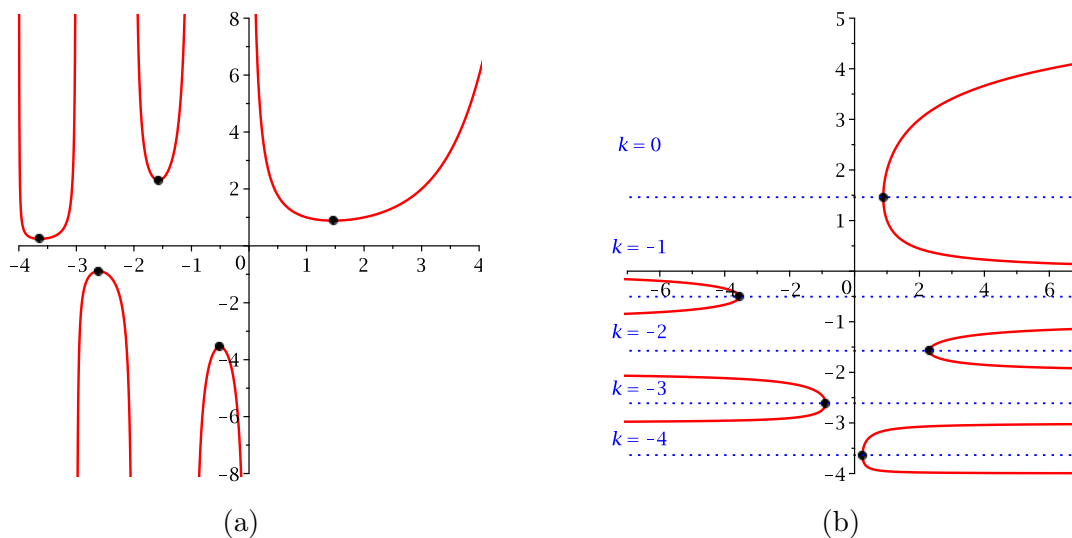


Figure 2.1: (a) Real-valued Γ .(b) Real-valued Inverse of Γ . Note the poles in Γ at non-positive integers become the critical points in $\check{\Gamma}$ where the branch changes. The ranges of the branches are shown labelled with k .

Figure 2.2 compares the principal branch to the \ln function. The Inverse Gamma function grows even more slowly than the \log function.

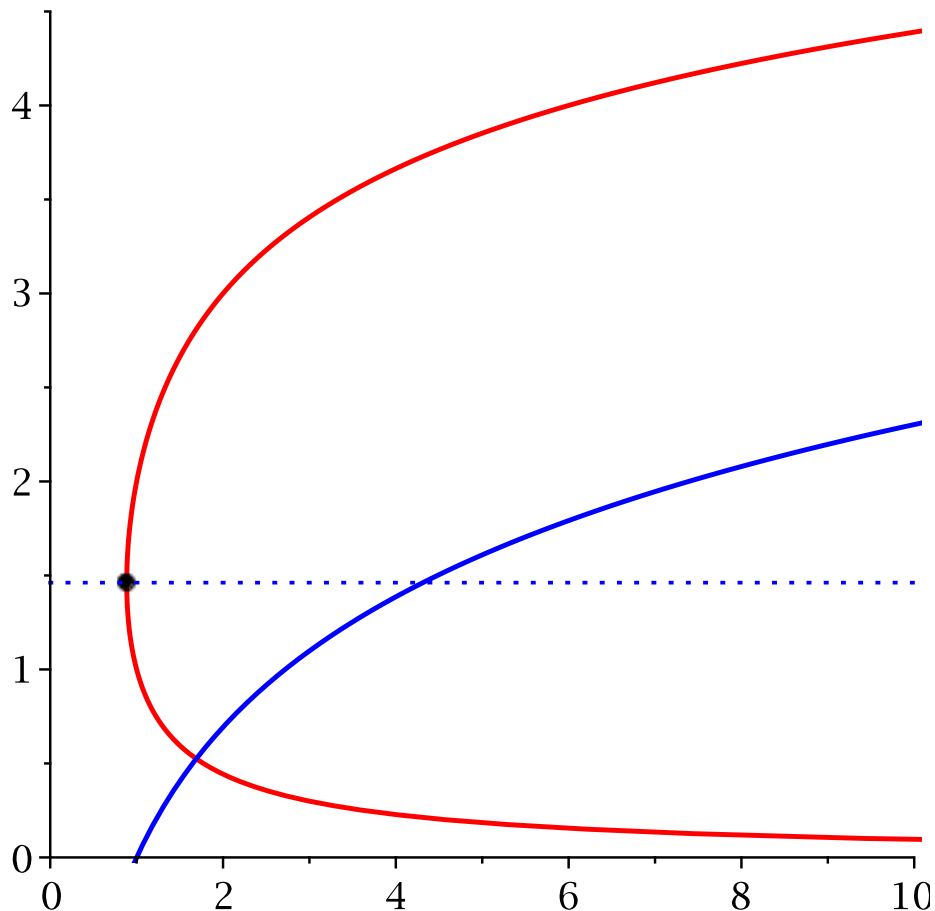


Figure 2.2: The principal branch $\check{\Gamma}_0$ (red) compared to the \ln function(blue). The \ln function grows faster than the principal branch. Note that the log function is placed below the principal branch, but will eventually overtake the Inverse Gamma function.

2.4 The condition number of the Inverse function

The condition number is a well-known parameter used to compare the stability of the evaluation of a function. In this section we show a method to plot the condition number of the Inverse of a function only using the function itself. Given any function $g(x)$, and a point x , the condition number C at x is defined [5] by

$$C(g, x) = \frac{xg'(x)}{g(x)} \quad (2.2)$$

Assume we know a function f and we want to plot, or calculate, the condition number for evaluating its inverse \check{f} . We write the function and its inverse as a pair of equations:

$$y = \check{f}(x) , \quad (2.3)$$

$$x = f(y) . \quad (2.4)$$

In our case, we want $C(\check{\Gamma}, x)$. We begin by recalling an elementary result. Differentiate the above equations w.r.t. x .

$$\frac{dy}{dx} = \frac{d\check{f}(x)}{dx} \quad (2.5)$$

$$1 = \frac{df}{dy} \frac{dy}{dx} \quad (2.6)$$

From the pair above and equation

$$\check{f}'(x) = \frac{d\check{f}(x)}{dx} = \frac{1}{df(y)/dy} \quad (2.7)$$

Therefore we have a parametric representation for the condition number:

$$C(\check{f}, x) = \frac{x\check{f}'(x)}{\check{f}(x)} = \frac{x}{(df/dy)\check{f}(x)} \quad (2.8)$$

$$= \frac{f(y)}{(df/dy)y} = 1/C(f, y) \quad (2.9)$$

From this we see we can treat y as a parameter, and specify the condition number using y as a parameter. Specializing this to the Γ function, we have

$$C(\check{\Gamma}, x) = 1/C(\Gamma, y) = \frac{1}{y\Psi(y)} , \quad (2.10)$$

$$x = \Gamma(y) . \quad (2.11)$$

To plot a parametric representation in Maple we use

```
plot([x(t),y(t),t=a..b])
```

So in the present case we have

```
plot([GAMMA(y),1/(y*Psi(y)),y=0.1..1.45])
```

Figure 2.3 shows the condition number for branch $\check{\Gamma}_0$. It is clear on the figure that the Inverse function is well conditioned except near the branch points.

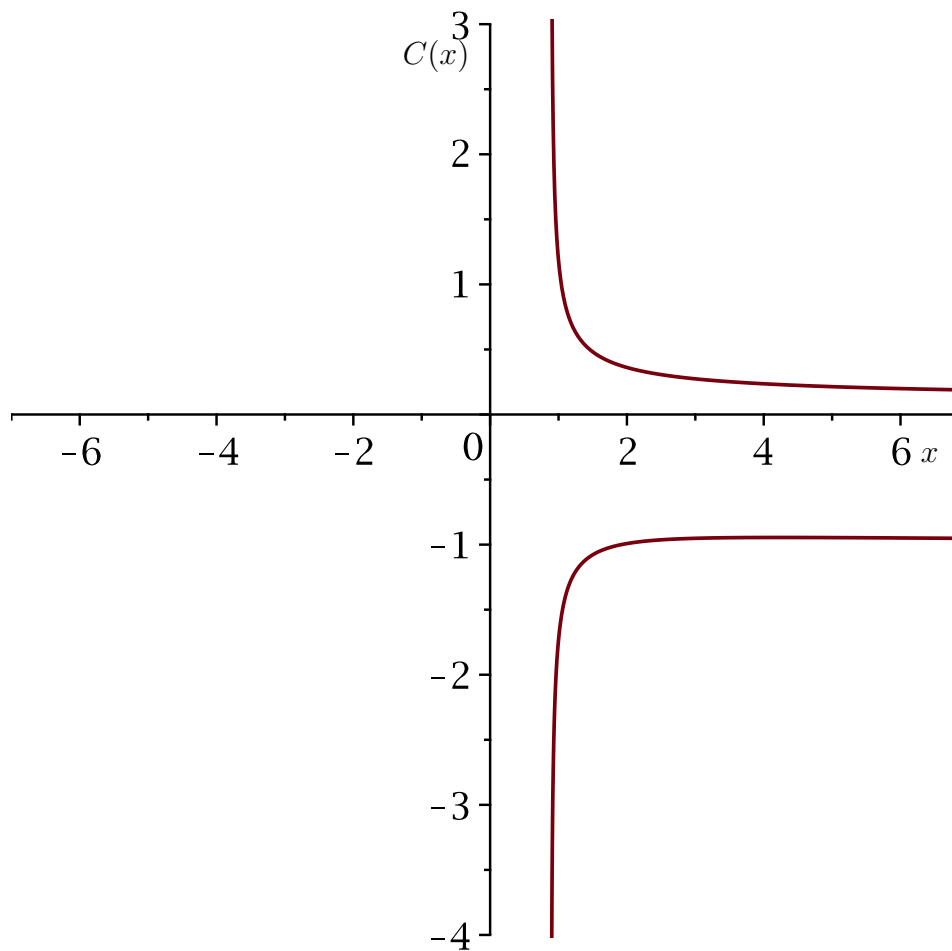


Figure 2.3: The condition number of the inverse function of Γ . Eq. (2.10)

2.5 Estimates for the principal branch $\check{\Gamma}_0$

In this section, we explore and compare different approximation formulas for the principal branch $\check{\Gamma}_0$. We shall group the approximations based on the approximation of the Γ

function that is inverted to obtain the Inverse function of Γ . Following the branch numbering system we adopted earlier, the Principal branch $\check{\Gamma}_0$ of the Inverse function of Γ is defined for the real arguments in the interval $x > \gamma_0$ and the corresponding real range is $[\psi_0, \infty]$.

2.5.1 Stirling-based approximation

One of the first asymptotic approximation for the computation of $\check{\Gamma}_0$ is proposed in [1] and is based on the inversion of the original Stirling formula. It is defined by

$$y(x) \sim \frac{1}{2} + \frac{\ln(x/\sqrt{2\pi})}{W_0(e^{-1} \ln(x/\sqrt{2\pi}))} \quad (2.12)$$

This expression becomes complex for $x < e^{-1}\sqrt{2\pi} \approx 0.92$, but delivers a good starting approximation for $x > 1$ as we can see on figure 2.4. For $x < 1$, the approximation becomes poor and get worse as the argument gets closer to the turning point.

Another asymptotic approximation derived from the Stirling formula and suggested in

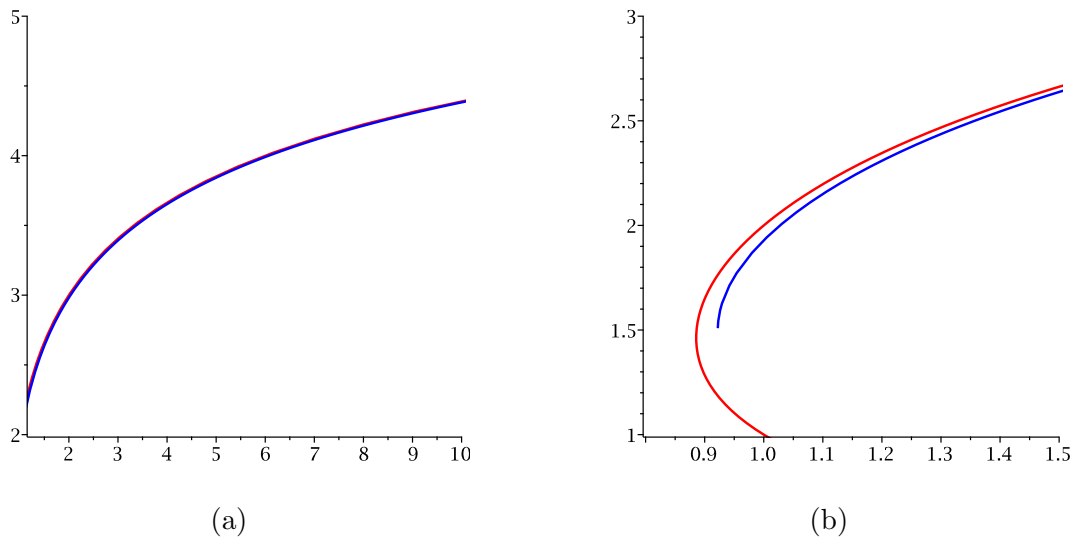


Figure 2.4: (a) $\check{\Gamma}_0(x)$ (red solid) and the approximation (2.12)(blue solid) for larger argument range.(b) For small argument range.

[1] is

$$y(x) \sim \frac{1}{2} + \frac{1}{24u_0(1+w)} - \frac{(5 + 10(1+w) + 14(1+w)^2)}{5760(1+w)^3u_0^3} + \dots \quad (2.13)$$

where $u_0 = \ln(x\sqrt{2\pi})/w$ with $w = W_0(\ln(x/\sqrt{2\pi})/e)$. Here again, the expression (2.13)

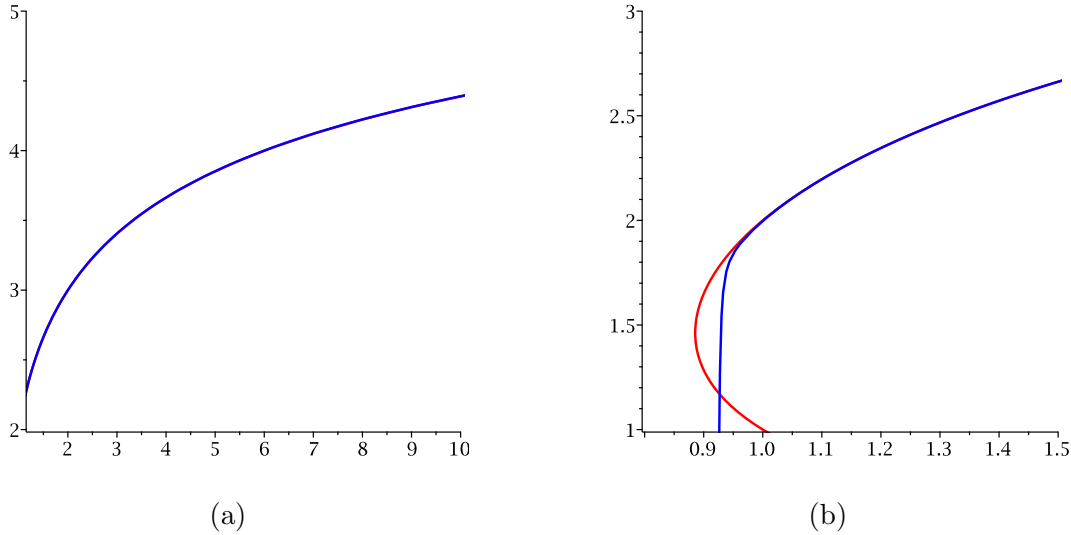


Figure 2.5: (a) $\check{\Gamma}_0(x)$ (red solid) and the approximation (2.13) (blue) .(b) For small argument range

delivers a good starting approximation for $x > 1$ as we can see on figure 2.5. Table 2.3 compares the approximation (2.13) and (2.12) for a few known arguments with the corresponding relative error $\frac{\check{\Gamma}_0 - y}{\check{\Gamma}_0}$. The error decreases for both approximations as the arguments becomes larger, but the error for (2.13) is much smaller than the that of the approximation (2.12) until value $x < 1$. It's around the turning point γ_0 that the expression (2.12) is better than the expression (2.13).

x	$\check{\Gamma}_0$	Eq. (2.12)/error	Eq. (2.13)/error
$\frac{\sqrt{\pi}}{2} = 0.88623$.	$3/2$	complex	complex
$\Gamma(1.8) = 0.93138$	1.8	1.64452./8.6%	1.60325./10.8%
$\Gamma(1.92321) = 0.96992$	1.92321	1.83429./3.6%	1.91500/0.4%
1	2	1.92884./3.6%	1.99700./0.2%
$\frac{3\sqrt{\pi}}{4} = 1.32934$.	$5/2$	2.47003/1.2%	2.49989./ $4.2 \times 10^{-5}\%$
$\frac{15\sqrt{\pi}}{8} = 3.32335$.	$7/2$	3.48741./0.4%	3.49999./ $1.5 \times 10^{-6}\%$
24	5	4.99386./0.1%	4.99999./0%

Table 2.3: Numerical values of $\check{\Gamma}_0(x)$, approximation (2.12) and (2.13)

2.5.2 Ramanujan-based approximation

In this section, we intend to derive a closed form estimate for the principal branch of the Inverse function of Γ by inverting the Ramanujan formula, [24]. The Ramanujan formula is defined by

$$\Gamma(y) \sim \sqrt{\frac{2\pi}{y}} \left(\frac{y}{e}\right)^y \left[1 + \frac{1}{2y} + \frac{1}{8y^2} + \frac{1}{240y^3} - \frac{11}{1920y^4} + \frac{79}{26880y^5} \dots\right]^{1/6}, \quad x \rightarrow \infty \quad (2.14)$$

inverting the above formula is not simple; we follow the method used in [1]. Applying \ln function to the above equation gives:

$$\ln \Gamma(y) \sim y \ln y - y + \ln \sqrt{2\pi} - \frac{1}{2} \ln y + \frac{1}{6} \ln K \quad (2.15)$$

where $K = 1 + \frac{1}{2y} + \frac{1}{8y^2} + \frac{1}{240y^3} \dots$. The series expansion of $\ln K$ in Maple using the command `Series(ln K,x,2)`, is

$$\ln K \sim -\ln(240) + \ln(1/y^3) \quad (2.16)$$

The above equation becomes

$$\ln \Gamma(y) \sim y \ln y - y + \ln \sqrt{2\pi} - \ln y - \ln 240/6 \quad (2.17)$$

We want to solve

$$x = \Gamma(y) \quad (2.18)$$

for y when x becomes large. Posing $v = x/\sqrt{2\pi}$, and $K1 = -\ln 240/6$, the equation (2.18) becomes

$$y \ln y - y - \ln y = \ln v - K1 \quad (2.19)$$

Dropping the term $\ln y$, the equation (2.19) becomes

$$y \ln y - y = \ln v - K1 \quad (2.20)$$

$$\frac{y}{e} \ln \frac{y}{e} = \frac{1}{e}(\ln v - K1) \quad (2.21)$$

$$\left(\ln \frac{y}{e}\right) e^{\ln y/e} = \frac{1}{e}(\ln v - K1) \quad (2.22)$$

Using the Lambert W function,

$$\ln \frac{y}{e} = W\left(\frac{1}{e}(\ln v - K1)\right) \quad (2.23)$$

and

$$\frac{y}{e} = e^{W\left(\frac{1}{e}(\ln v - K1)\right)} = \frac{\frac{1}{e}(\ln v - K1)}{W\left(\frac{1}{e}(\ln v - K1)\right)} \quad (2.24)$$

given

$$y = \frac{\ln(x/\sqrt{2\pi}) - K1}{W\left(\frac{1}{e}(\ln(x/\sqrt{2\pi}) - K1)\right)} \quad (2.25)$$

Figure 2.6 shows that the expression (2.25) is far from delivering a good starting value for the principal branch $\check{\Gamma}_0$ even asymptotically as it was the case for the two previous approximations. But at least, the graph of the approximation (2.25) seemed to have the same slope as the graph of $\check{\Gamma}_0$, suggesting that any simple iterative scheme might help to improve the solution.

2.6 Iterative Schemes

The three approximations formulae we investigated so far are obtained by inverting a particular Γ approximation, by solving the equation $\Gamma(y) = x$ for y . This suggests that an iterative scheme can be used to improve the solution given an initial estimate. In this section we test a few, well-known iterative schemes and compare the solution for small arguments x . Some considerations we shall keep in mind that affect the efficiency of any

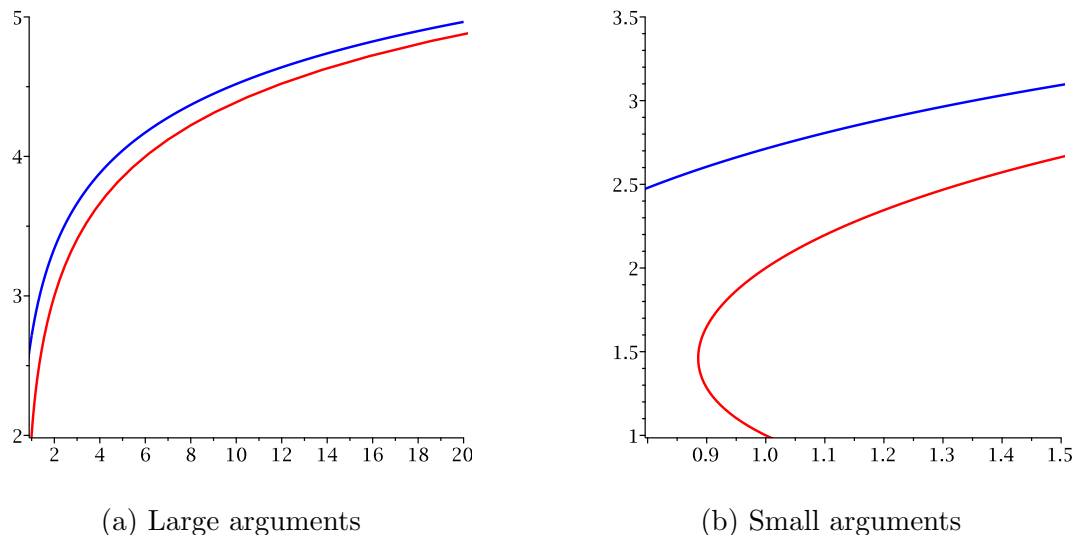


Figure 2.6: (a) $\check{\Gamma}_0(x)$ (red solid) the approximation (2.25) (blue solid). (b) For small argument range.

iterative schemes are:

- Cost of initial estimate. More time spent on obtaining a better estimate can reduce the number of iterations.
- Cost of an iteration. This is affected by the choice of the function used for the iteration, and the order. Maple has implemented both a `GAMMA` function and a `lnGAMMA` function. Either could be used for the iteration.
- The order of the iteration scheme. By using a higher-order scheme, one can reduce the number of iterations.

2.6.1 Newton Schemes

To solve $\Gamma(y) - x = 0$ for y , given an initial approximation y , the Newton procedure in Maple is

```
Newton:= proc(y,x) local Gtmp,f,fprime;
Gtmp:= G(y);
f:= Gtmp - x;
```

```
fprime := Psi(y)*Gtmp;
return y-f/fprime;
end proc;
```

Below, we rewrite the three closed form formula for the Principal branch $\check{\Gamma}_0$

$$y(x) \sim \frac{1}{2} + \frac{\ln(x/\sqrt{2\pi})}{W_0(e^{-1} \ln(x/\sqrt{2\pi}))} \quad (2.26)$$

$$y(x) \sim \frac{1}{2} + \frac{1}{24u_0(1+w)} - \frac{(5 + 10(1+w) + 14(1+w)^2)}{5760(1+w)^3 u_0^3} + \dots \quad (2.27)$$

where $u_0 = \ln(x\sqrt{2\pi})/w$ with $w = W_0(\ln(x/\sqrt{2\pi})/e)$.

$$y(x) \sim \frac{\ln(x/\sqrt{2\pi}) - K1}{W\left(\frac{1}{e}(\ln(x/\sqrt{2\pi}) - K1)\right)} \quad (2.28)$$

We solve the $\Gamma(y) - x = 0$ for two arguments range, for $x = 0.93$ and $x = 1$ given an initial estimate from the three above formulas. Table 2.4 and 2.5 shows the backward error at each iteration. The error decreases for all three approximates of $\check{\Gamma}_0$ but the

k	Eq. (2.26)	Eq. (2.27)	Eq. (2.28)
0	3.2×10^{-2}	4.2×10^{-2}	5.4×10^{-1}
1	2.1×10^{-2}	2.1×10^{-1}	1.5×10^{-1}
2	1.7×10^{-3}	4.6×10^{-2}	3.0×10^{-2}
3	1.5×10^{-5}	5.9×10^{-3}	3.1×10^{-3}
4	1.3×10^{-9}	1.7×10^{-4}	4.9×10^{-5}
5	0	1.7×10^{-7}	1.4×10^{-8}
6	0	0	0

Table 2.4: Error for solving $\Gamma(y) - 0.93$ for y given an initial y_0

approximation (2.26) outperform the other two by reducing the error by a factor of between 10 to 10^4 within 4 iterations for $x = 0.93$. But for $x = 1$, the approximation (2.27) gives a better approximates of $\check{\Gamma}_0$. In table 2.4, the initial error of the approximation (2.26) is $\text{err} \sim 0.032$, which is slightly smaller than the $\text{err} \sim 0.042$ of the approximation 2.27, resulting in less iterations. This confirms the result we had in the last section while

k	Eq. (2.26)	Eq. (2.27)	Eq. (2.28)
0	2.8×10^{-2}	1.3×10^{-3}	5.6×10^{-1}
1	2.4×10^{-3}	3.7×10^{-6}	1.4×10^{-1}
2	1.3×10^{-5}	0	2.2×10^{-2}
3	0	0	9.5×10^{-4}
4	0	0	2.1×10^{-6}
5	0	0	0

Table 2.5: Error for solving of $\Gamma(y) - 1$ for y given an initial y_0

using the relative error $(\check{\Gamma}_0 - y)/\check{\Gamma}_0$ as a comparison parameter, that is the approximation (2.27) is better than the approximation (2.26) for all argument except around the turning point $x \sim e^{-1}\sqrt{2\pi}$ where (2.26) does better. In both argument interval, the expression (2.28) demands more iterations. The estimate to choose from depends on the arguments range. The iterative scheme is effective to reduce the number of iteration only when a better starting estimate is given.

2.6.2 Inverse Quadratic Interpolation

Inverse Quadratic Interpolation is an iterative scheme like Muller's scheme, [26],² that uses three previous points to extrapolate the next point. But unlike Muller's method, Inverse Quadratic Interpolation interpolates the three points with a quadratic inverse function. To solve $\Gamma(y) - x = 0$, for y given three initial estimates y_0 , y_1 , y_2 , the IQI iteration is

```

IQI:= proc(y0,y1,y2,y3) local x;
f := G(y) - x;
y:= polyinterp([f(y0),f(y1),f(y2)], [y0,y1,y2], 0);
y0 := y1;
y1 := y2;
y2 := y;
return y;

```

²Page 50 of the reference

k	Newton	IQI
0	4.2×10^{-2}	4.2×10^{-2}
1	2.1×10^{-1}	1.9×10^{-2}
2	4.6×10^{-2}	3.2×10^{-3}
3	5.9×10^{-3}	4.0×10^{-4}
4	1.7×10^{-4}	1.3×10^{-6}
5	1.7×10^{-7}	1.2×10^{-10}
6	0	0

Table 2.6: Newton and Inverse Quadratic Interpolation for solving $\Gamma(y) - 0.93$ for y

end proc:

The problem with IQI is that it requires $f(y_0), f(y_1), f(y_2)$ to be distinct. The only approximation of $\check{\Gamma}_0$ that can guarantee that is the expression (2.27). The three starting points will be set as follows

$$\begin{aligned}
 y_0 &= \frac{1}{2} + u_0 \\
 y_1 &= y_0 + \frac{1}{24u_0(1+w)} \\
 y_2 &= y_1 + \frac{(5 + 10(1+w) + 14(1+w)^2)}{5760(1+w)^3u_0^3}
 \end{aligned} \tag{2.29}$$

where $u_0 = \ln(y/\sqrt{2\pi})/w$, with $w = W_0(\ln(y/\sqrt{2\pi})/e)$.

Table 2.6 compared the IQI and the Newton's schemes for solving $\Gamma(y) - 0.93$ given an initial estimate (2.27). Starting from the same value, $\epsilon \approx 4.2 \times 10^{-2}$, the error of IQI scheme is 10 times smaller than that of Newton's scheme for the first iterations. And from the fourth iteration, the error becomes 100 to 1000 times smaller. This shows that the choice of the iteration scheme can drastically impact the error rate or the number of iterations before convergence, assuming we have a good initial estimate.

2.6.3 Improving the estimates for small arguments

We saw earlier that all the approximations deliver good starting values for $x > 1$ but do poorly for $x < 1$ and around the turning points $\gamma_0 = \Gamma(\psi)$. A simple method will be to

use a Taylor series around the turning point $x = \gamma_0$. For $\gamma_0 \leq x \leq 1$ the Taylor series around γ_0 is

$$\Gamma(y) = \gamma_0 + \frac{1}{2}\gamma_0\Psi(1, \psi_0)(y - \psi_0)^2 + O((y - \psi_0)^3) , \quad (2.30)$$

where the linear term is absent because we expand around a stationary point. Given a specific value x of $\Gamma(y) = x$ for which we need the inverse, we solve the equation (2.30) for y by dropping the error term and solving the quadratic equation:

$$y \sim \check{\Gamma}_0(x) = \psi_0 + \sqrt{\frac{2(x - \gamma_0)}{\Psi(1, \psi_0)\gamma_0}} . \quad (2.31)$$

The principal branch is given by the positive square root. As we can see on figure 2.7, there more agreement between the approximation (2.31) and $\check{\Gamma}_0$ than (2.26) and $\check{\Gamma}_0$. Numerical values in table 2.7 shows that around the turning point γ_0 , the Taylor equation gives a better starting approximation than both the expression 2.26 and 2.27.

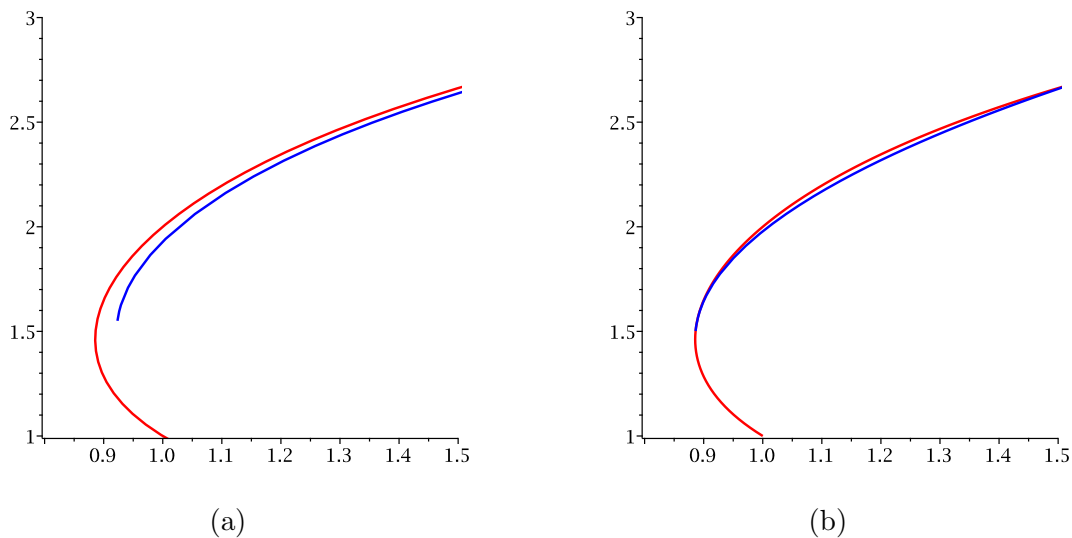


Figure 2.7: (a) Estimates around the turning point γ_0 for approximation (2.26), (b) Estimates around the turning point γ_0 for approximation (2.31)

x	$\tilde{\Gamma}_0$	Eq. (2.26)/error	Eq. (2.27)/error	Eq. (2.31) /error
$\frac{\sqrt{\pi}}{2} \approx 0.886$	3/2	complex	complex	1.5003/0.02%
$\Gamma(1.8) \approx 0.9314$	1.8	1.6445/8.6%	1.603/10.8%	1.788/0.63%
$\Gamma(1.92321) \approx 0.9699$	1.923	1.8343/3.6%	1.915/0.4%	1.9052/0.94%
1	2	1.9288/3.6%	1.9970/0.2%	1.9783/1.1%
$\frac{3\sqrt{\pi}}{4} \approx 1.3293$	5/2	2.4700/1.2%	2.4999/ $4.2 \times 10^{-5}\%$	2.4793/0.83%
$\frac{15\sqrt{\pi}}{8} \approx 3.3234$	7/2	3.4874/0.4%	3.4999/ $1.5 \times 10^{-6}\%$	3.8468/10%
24	5	4.9939/0.1%	4.9999/0%	8.8063/76%

Table 2.7: Numerical values of approximation (2.12) and approximation (2.13)

2.6.4 The rate of convergence near the turning point γ_0

It is well known that near a stationary point, Newton's method degrades from quadratic convergence to linear convergence. Consequently, near $x = \gamma_0$, we explore a quadratic scheme³. We expand around an initial estimate:

$$\Gamma(a) + \Psi(a)\Gamma(a)(x - a) + 1/2\Gamma(a)(\Psi'(a) + \Psi(a)^2)(x - a)^2 + O((x - a)^3) \quad (2.32)$$

where Ψ' is the derivative of the Ψ function. Solving for x gives the iterative scheme below. To solve $\Gamma(y) - x = 0$, given an initial estimate y , the Maple iteration is

```

QS := proc (y, x) local dx, a, b, c;
a := (1/2)*(Psi(1, y) + Psi(y)^2*G(y));
b := Psi(y)*G(y);
c := G(y)-x;
dx := (1/2)*(-b + sqrt(b^2 - 4*a*c))/a;
return y + dy;
end proc;
```

Table 2.8 shows the number of iterations needed by Newton's method and the quadratic scheme near the stationary point $x = \gamma_0$. There is a gain of, at most, two iterations for

³Note that we are not using a similar scheme called Muller's method, nor the Inverse Quadratic Iteration, which do not require the evaluation of derivatives [26]

x	NM	QS
1.000	4	2
0.950	3	2
0.900	3	2
0.890	3	2
0.886	3	1

Table 2.8: Number of iterations near $x = \gamma_0$ for branch $k = 0$. The starting estimate was based on Eqn (2.31). The columns correspond to Newton's method (NM) and our quadratic scheme (QS). The iteration was continued until the relative error was less than 10^{-16}

the quadratic scheme over the Newton scheme, but this comes with a drawback in that one must explicitly evaluate the second derivative of $\Gamma(y) - x$ and extract a square root.

2.7 Estimates for the branch $\check{\Gamma}_{-1}$

The branch $k = -1$ or $\check{\Gamma}_{-1}(x)$ has two real domains and two associated ranges: The positive real domain $[\gamma_0, \infty]$ and its positive range $[0, \psi_0]$; and the negative domain $]\infty, \gamma_{-1}[$ has its negative range $]\psi_{-1}, 0[$. The first approximation for positive domain of this branch is proposed in [1] who uses the second branch of the Lambert W function

$$y(x) \sim \frac{1}{2} + \frac{\ln(x/\sqrt{2\pi})}{W_{-1}(e^{-1} \ln(x/\sqrt{2\pi}))} \quad (2.33)$$

Another approximation is proposed in [7]

$$y(x) \sim \frac{1}{x} \quad (2.34)$$

Figure 2.8 shows the branch $\check{\Gamma}_{-1}(x)$ and the two approximation. The estimate (2.12) seemed to be a better starting point for the branch for small arguments range than the estimate (2.34), but it's only defined for $x \in [\frac{\sqrt{2\pi}}{e}, \sqrt{2\pi}]$. The approximation (2.34), on the other hand is defined on the whole real line. It agrees with the branch as the arguments become larger. As with the principal branch $\check{\Gamma}_0$, one can use the Taylor series

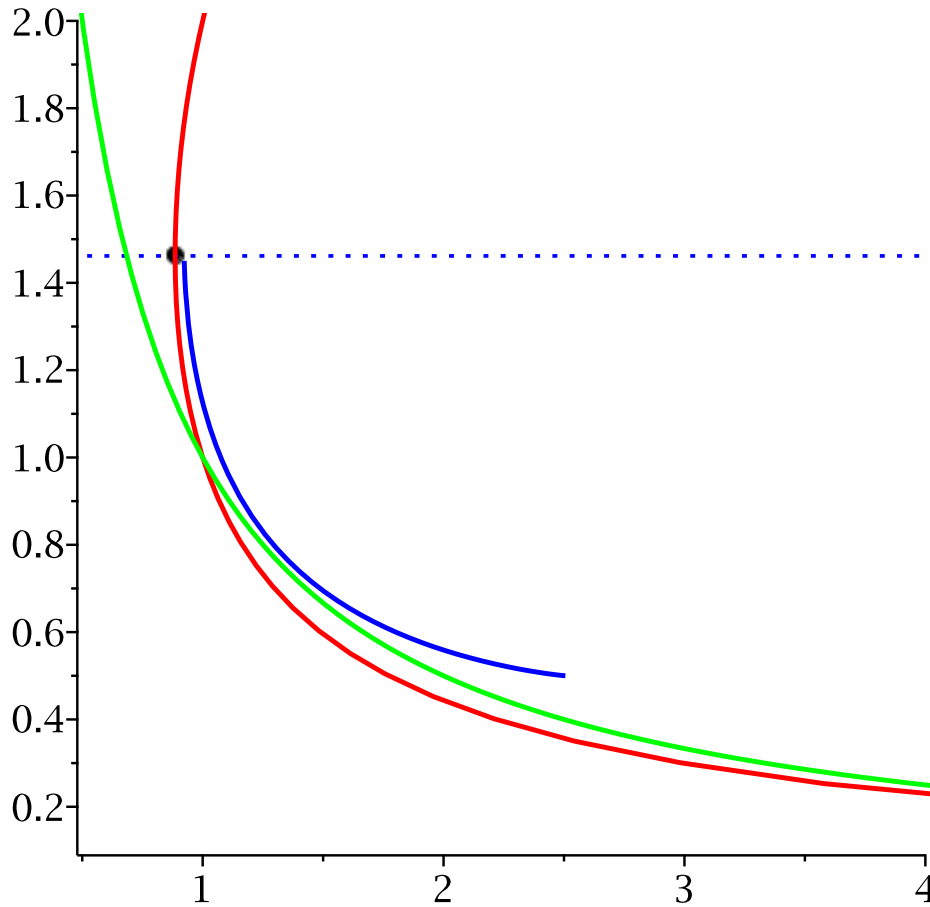


Figure 2.8: $\check{\Gamma}_{-1}(x)$ (solid red), the approximation 2.33(blue solid) and 2.34(solid green)

in the interval $\gamma_0 \leq x \leq 1$ to have a better starting estimate. The Taylor series is defined by

$$y = \check{\Gamma}_{-1}(x) = \psi_0 - \sqrt{\frac{2(x - \gamma_0)}{\Psi(1, \psi_0)\gamma_0}} \quad (2.35)$$

Table 2.9 shows some particular numerical values of the expression (2.12), (2.34) and (2.35).

x	$\check{\Gamma}_{-1}$	Eq. (2.33)/error	Eq.(2.34)/error	Eq.(2.35)/error
γ_0	ψ_0	complex	1.1292 /22%	1.4616 / 0%
1	1	1.1254 /11%	1 / 0%	0.945/5.5%
$\Gamma(0.8) = 1.1642$	0.8	0.900/ 12.5%	0.8589 / 7.4%	0.6552 / 18%
$\sqrt{\pi}$	1/2	0.6072 / 21%	0.5641 /12%	0.0229/96%

Table 2.9: Numerical values of the approximation (2.12), (2.34) and (2.35)

2.8 Estimates for other branches $\check{\Gamma}_k$

The other branches of $\check{\Gamma}_k$ can be obtained with the same procedure.

- Expand $\Gamma(y)$ around the singular point.
- Keep only one term of the expansion.
- Invert the expansion, by solving $\Gamma(y) - x = 0$ for y . The result is the initial approximation of the branch
- Use an iterative scheme to improve the solution

Figure 2.9 shows the approximation of the branch $\check{\Gamma}_{-2}$ and $\check{\Gamma}_{-3}$. The question is how many

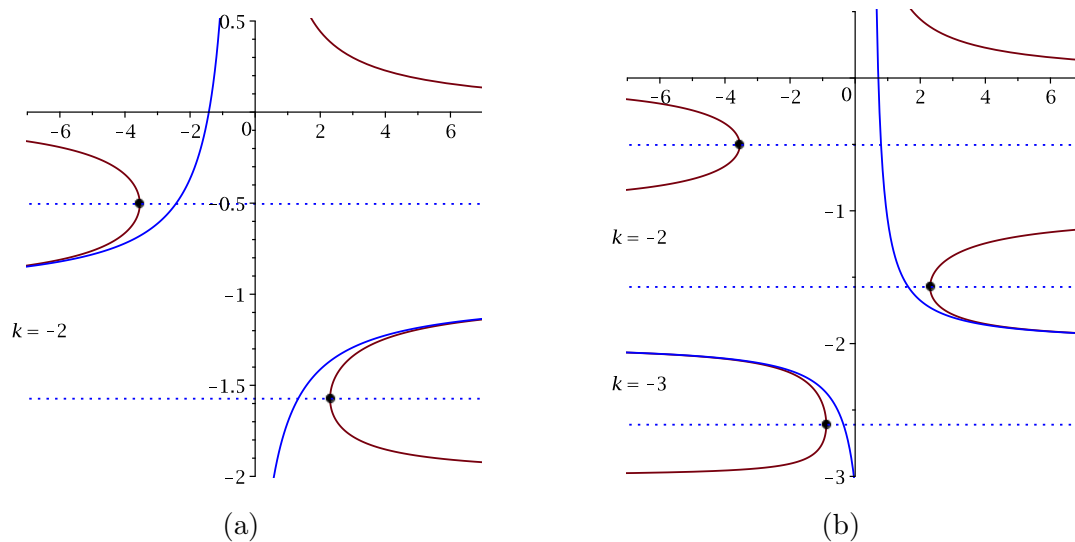


Figure 2.9: (a) The branch $\check{\Gamma}_{-2}(x)$. The branch $\check{\Gamma}_{-3}(x)$

branches can we really compute? Not many. As we seek to compute more branches, the turning points $\gamma_k = \Gamma(\psi_k)$ become smaller and the and as a consequence $\check{\Gamma}_k(x) \rightarrow$ the pole of $\Gamma(x)$

2.9 Conclusion

In this chapter, we explored three different approximations for the numerical computation of real-valued $\check{\Gamma}_k(x)$. Numerical values and the plots show that these approximations

deliver good starting points for the branches $\check{\Gamma}_k(x)$ for large argument range but underperformed for small arguments. We also show that, once we have a good starting estimate, an iterative scheme can be used to improve the solution and we compared two iterative schemes for that matter. Finally, we showed that the estimate to choose from depends on the arguments range. In the next chapter, we will focus on the extension of $\check{\Gamma}_k(z)$ in the complex plane.

Chapter 3

Complex Inverse function of Γ

3.1 Introduction

The idea of extending the Inverse function of $\Gamma(x)$ in the complex plane was first introduced by M. Uchiyama in his paper, [23]. He proved that the principal inverse of Γ restricted to the interval $[\alpha, \infty]$ denoted as $\Gamma^{-1}(x)$ has the holomorphic extension $\Gamma^{-1}(z)$ to the cut plane $\mathbb{C} \setminus]-\infty, \Gamma(\alpha)]$, where α is the unique zero of the logarithmic derivative Ψ of $\Gamma(x)$ on the positive half real line. Moreover, [23] showed the extension $\Gamma^{-1}(z)$ is a Pick function. In [19], the authors got the same result as [23] but on the decreased interval $[0, \alpha]$. Both [23] and [19] based their proof on the Löwner theorem that relates the positive semi-definite Löwner kernel to a Pick function. In the last Chapter, we reviewed some properties of the Inverse function of $\Gamma(x)$ in the real domain. In this chapter, we shall extend the Inverse function $\Gamma(x)$ in the complex plane using the technique introduced by David J. Jeffrey in [11].

3.2 Notation

Throughout this chapter, the Inverse function of $\Gamma(x)$ will be denoted by $\check{\Gamma}_k(x)$ in real domain and by $\check{\Gamma}_k(z)$ in the complex plane, where k denotes the branch number.

3.3 The extension of $\check{\Gamma}_k(x)$ to the complex plane

We shall extend the $\check{\Gamma}_k(x)$ function in the complex plane using the technique in [11]. We describe the general technique first. Let us say we want to extend the real-valued function $y = f(x)$ in the complex plane. The technique in [11] can be summarized as follows.

- Denote the desired extension by $w = f(z)$.
- Plot side by side, the real z -domain and the real w -range of f .
- Starting from the real line in the w -range of f , draw a series of lines parallel to the imaginary axis.
- Map these parallel lines into the z -domain of f using the map $w \mapsto g(w)$, where $g(w)$ is the inverse function of $f(z)$.
- Trim the parallel lines in w -range so that their images do not collide in z -domain, but at the same time fill the z -domain.
- The line along which the images collide in the z -domain is a candidate for the branch cut.
- Note the range of $f(z)$ in the complex plane. Figure 3.1 shows the z -domain and the w -range of the mapping in the complex plane.

In the next section, we shall prepare the use of the technique in [11] with the examples of the $\log(x)$ function and the $\arcsin(x)$ function.

3.3.1 The extension of the log function in the complex plane

It's well-known that the $\log z$ function is a multivalued function and its inverse is the $\exp(z)$ function. We also know as a fact that $\log(x)$ defined on $[0, \infty]$ has a holomorphic extension $\log(z)$ to the cut plane $A = \mathbb{C} \setminus]-\infty, 0]$.

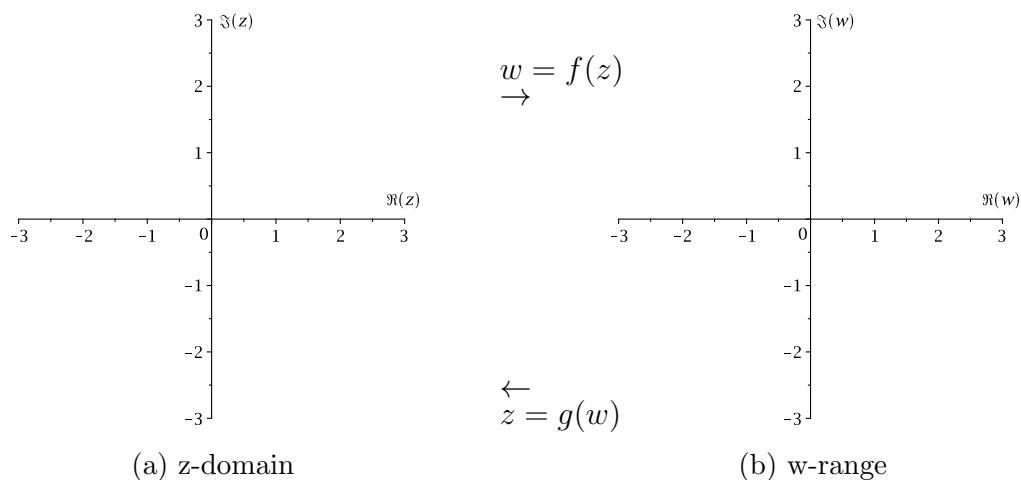


Figure 3.1: Domain and range for complex function mapping in the complex plane

The $\log z$ function is defined as

$$\begin{aligned} \log(z) &= \log |z| + i \arg(z) \quad z \neq 0 \\ &= \log |z| + i \text{Arg}(z) + 2\pi im, \quad m = 0, \pm 1, \pm 2, \dots, \quad -\pi < \text{Arg}(z) \leq \pi \end{aligned} \quad (3.1)$$

The value of $\log z$ are complex numbers w , such that $z = \exp(w)$.

The principal value is defined as

$$\text{Log}(z) = \log |z| + i \text{Arg}(z), \quad -\pi < \text{Arg}(z) < \pi. \quad (3.2)$$

To extend $\log(x)$ to the complex plane with the technique described in [11], starting from the real line, we extend the range $]-\infty, \infty[$ of $\log(x)$ into the complex domain by drawing a series of the straight contours parallel to the imaginary axis. The straight contours are mapped back to the z -domain using the map $w \mapsto e^w$. The image of the straight lines collide along the negative real axis in the z -domain. The intersection is not visible on figure 3.2 because the principal value and the other branches of the $\log(z)$ function have the same algebraic form, they only differ by $\pm 2\pi$.

Although [11] uses lines parallel to the imaginary axis, this is not necessary. If we use instead lines that slope, we can see the process more clearly. This is shown in figure

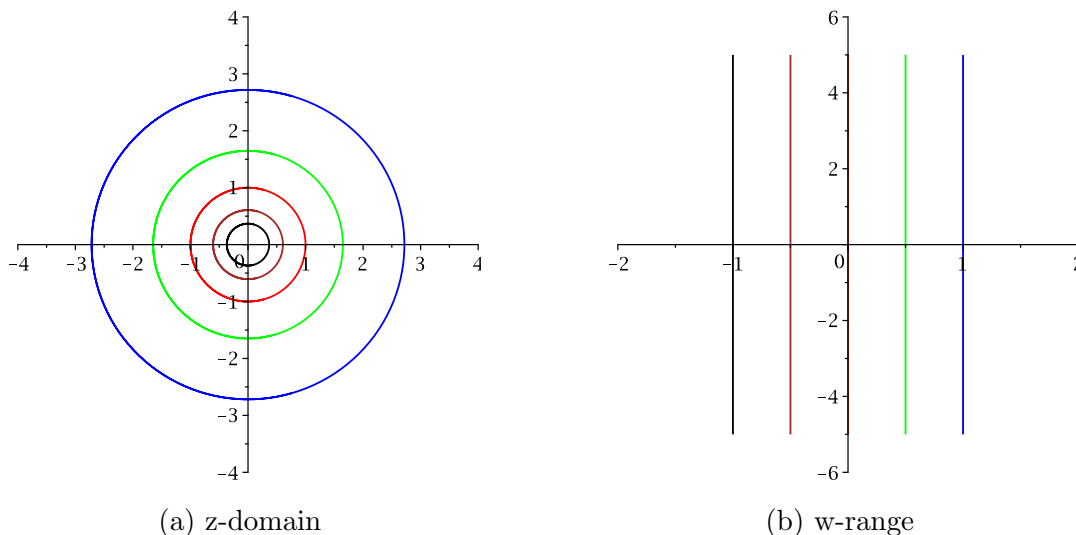


Figure 3.2: Extending the $\log(x)$ function into the complex plane. The straight contours are trimmed in w -range so that their images do not collide in the z -domain

3.3, where the collisions can be seen because the contours (now spirals) are passing themselves. To obtain the principal value of $\log(z)$, we must trim them on the imaginary

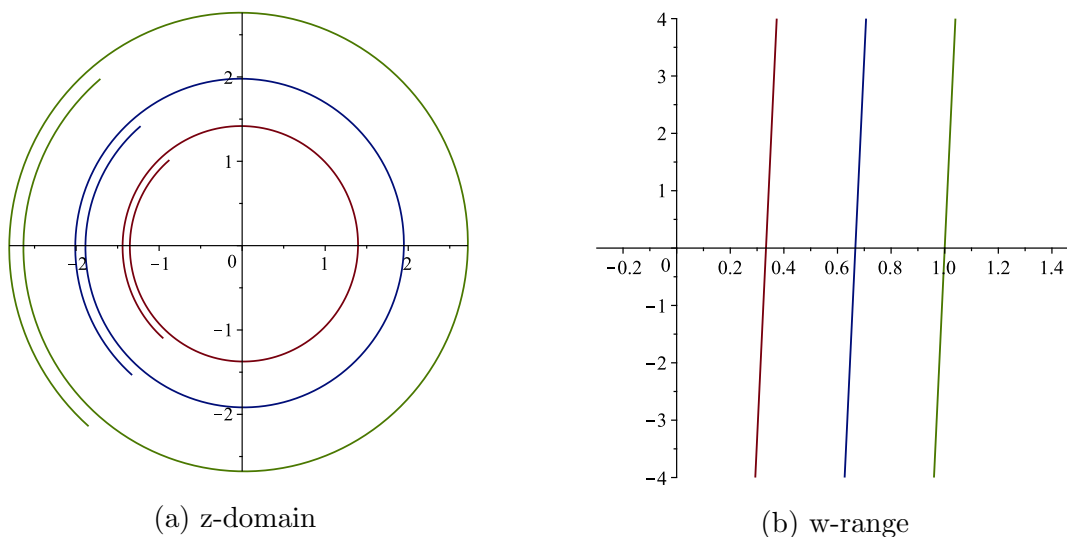


Figure 3.3: Extending the $\log(x)$ function into the complex plane. The straight contours are trimmed in w -range so that their images do not collide in z -domain. Adding the slight slope to the lines makes the collision easier to see.

axis at a point such that $-\pi < \Im(w) < \pi$. Figure 3.4, shows the range of the principal value defined as $\{\Re(w) = \log|z|, \pi < \Im(w) < \pi\}$. The other branches of $\log(z)$ are now

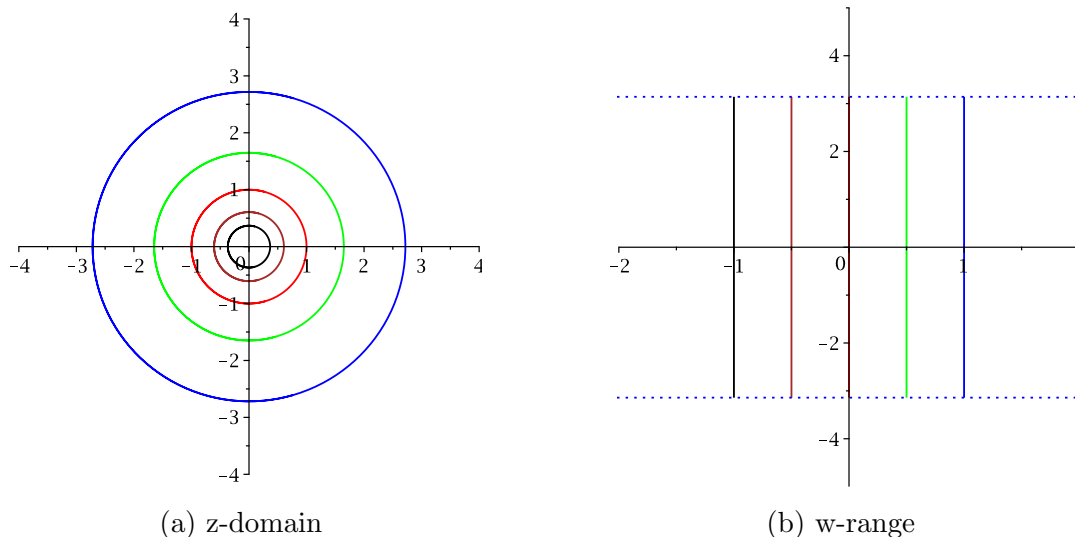


Figure 3.4: The range of the Principal value $\log z$ in the complex plane.

denoted [10] by $\ln_k z$, where k is the branch number. In algebraic terms, the definition is

$$\ln_k(z) = \text{Log}(z) + 2\pi ik . \quad (3.3)$$

In graphical terms, the procedure now is to remove from the w plane the region assigned to the principal branch, and repeat the construction of the two sets of contours in the remaining space. Figure 3.5 shows the range of $\ln_1 z$, where the contours have been trimmed to the region defined by $\pi < \Re(z) \leq 3\pi$.

3.3.2 The extension of the arcsin function in the complex plane

In this section we show another aspect of using contours to visualize branches. The inverse sine function is periodic in the real direction, different from the logarithm function which is periodic in the imaginary direction. If we use straight lines parallel to the imaginary axis, we do not get collisions. The sine function has a period of 2π , but an antiperiod¹ [13] of π radians. Therefore we start with the real interval in the w -range $[-\pi/2, \pi/2]$. We obtain the plots in figure 3.6. The branch cuts are clearly $|x| \geq 1$. The definition

¹ $f(x + T) = -f(x)$.

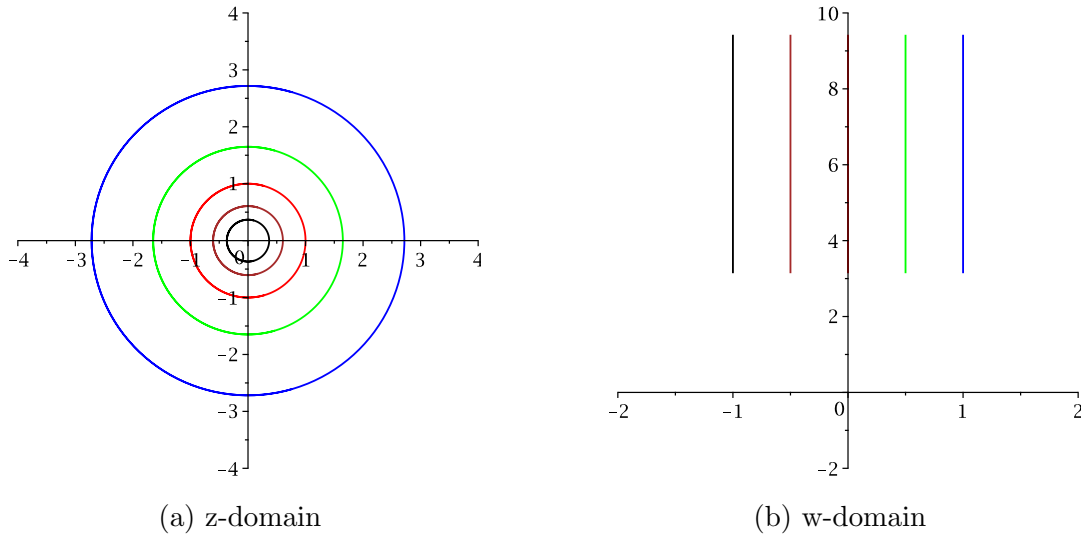


Figure 3.5: The range of the branch $k = 1$ of $\log(z)$ in the complex plane, denoted $\ln_1 z$.

of the branch cuts can also be seen using colliding contours, as was done for logarithm. This is shown in figure 3.7, where contours parallel to the real axis are used.

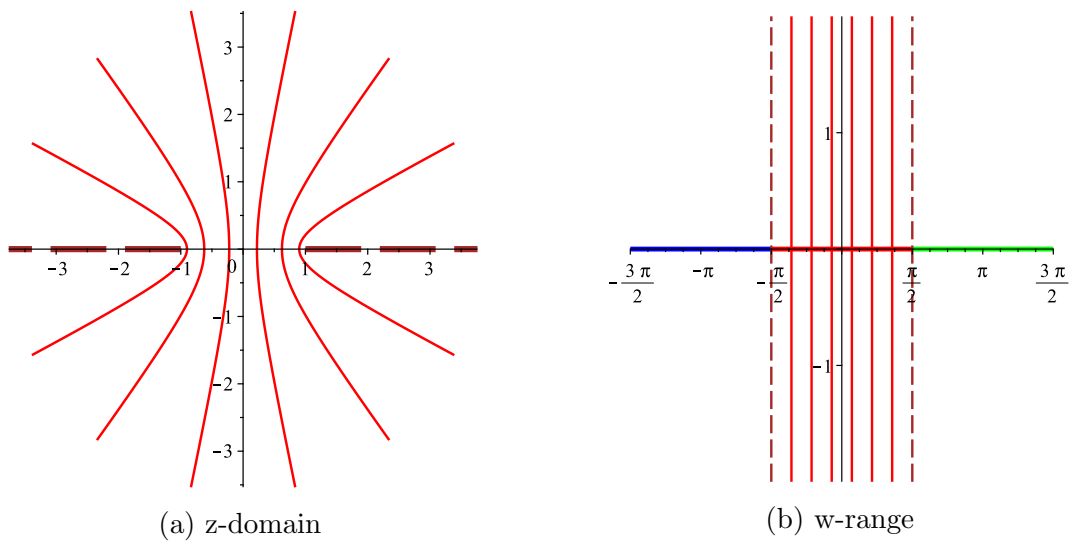


Figure 3.6: Extending the $\arcsin(x)$ function into the complex plane. The straight contours do not need to be trimmed in w -range, and yet the images show the branch cuts clearly.

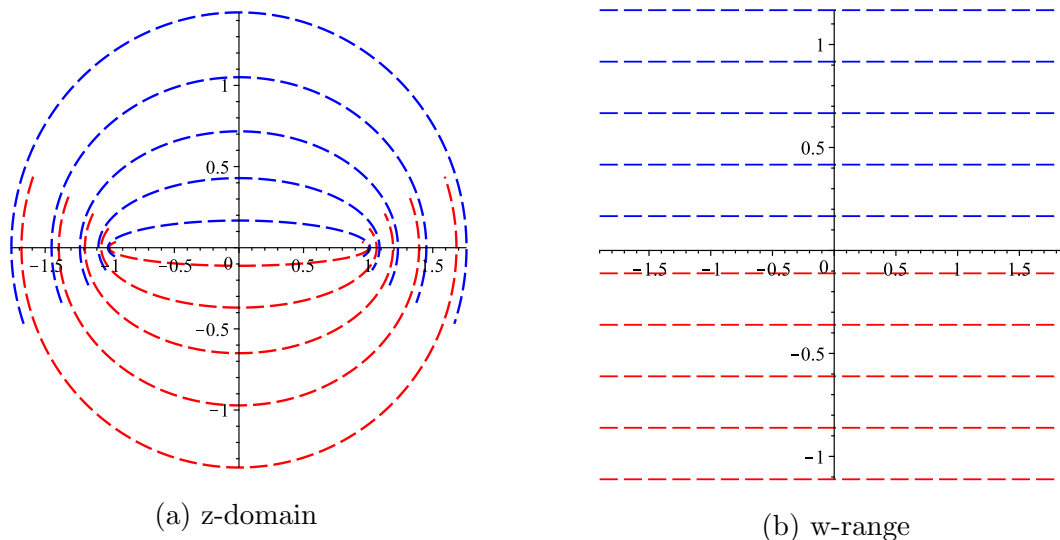


Figure 3.7: Extending the $\arcsin(x)$ function into the complex plane. The straight contours above the real axis in the z -domain have been slightly offset relative to those below the axis, so that the collisions are easily seen.

3.3.3 The extension of the $\check{\Gamma}_0$ in the complex plane

The real domain of the principal branch $\check{\Gamma}_0$ is the interval $[\gamma_0, \infty]$ and the range $[\psi_0, \infty]$, where $\gamma_0 = \Gamma(\psi_0)$ and ψ_0 is the positive zero of $\Gamma'(x)$. Following the same process and using the map $w \mapsto \Gamma(w)$, we get figure 3.8 that shows the images colliding on the negative real line in the interval $[-\infty, \Gamma(\psi_0)]$. Figure 3.9 is a zoom of figure 3.8(a) so

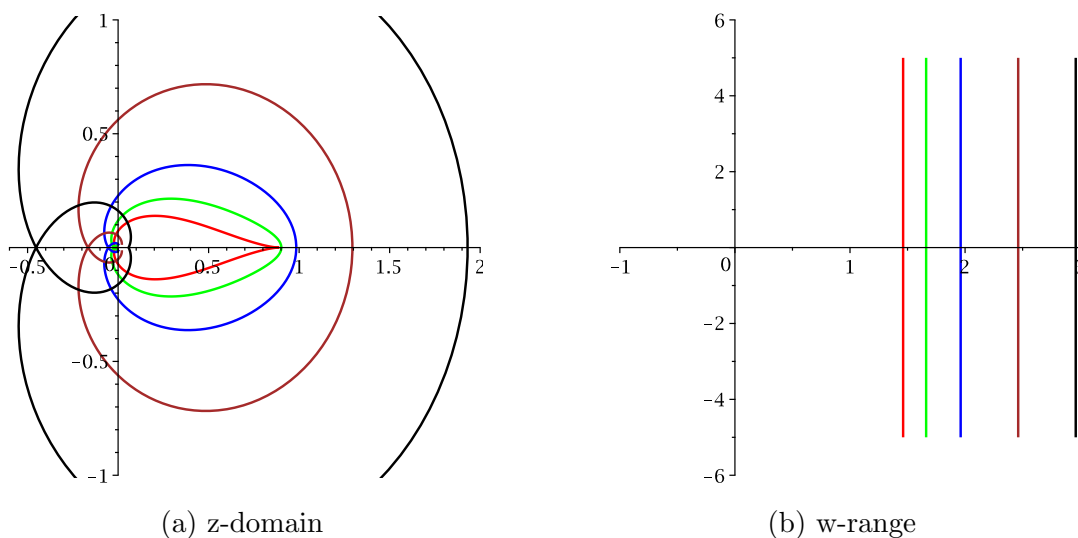


Figure 3.8: Extending the Principal branch of the inverse of $\Gamma(z)$ into the complex plane

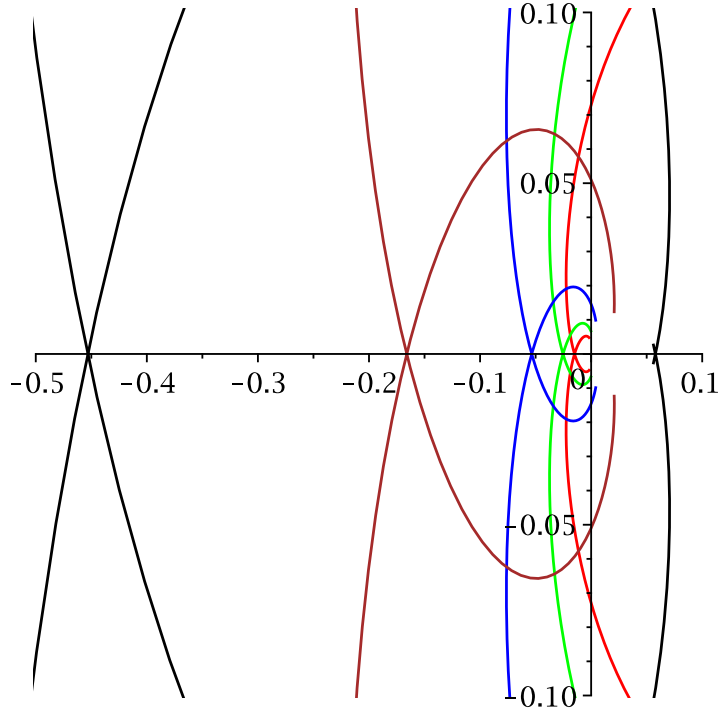


Figure 3.9: Zoom of 3.8(a)

that we can clearly see the intersection in the z -domain. Continuing with the process, the straight contours must be trimmed in the w -domain. The question is at what point w to trim in w -range. This is purely done, at this level, by a simple experimentation. The contours are trimmed at some random imaginary points and then mapped into the z -domain. If the image crosses the line of discontinuity, the line are shorten further in the w -range. This is not an automatic way of doing things but it does help in appreciating the range of the branches. Figure 3.10 shows the range of the principal branch $\check{\Gamma}_0$ in the complex plane. The interval $[-\infty, \gamma_0] = [-\infty, \Gamma(\psi_0)]$ is the branch cut. Figure 3.10 also shows that as the argument z becomes larger, the parallel lines become shorter. That's $\check{\Gamma}_0(z) \rightarrow \Re(\check{\Gamma}_0(z))$ as z becomes large. For complex numbers, z larger means the modulus of z is larger. This give three possible scenarios, the first is $\Re(z)$ is a big real number and $\Re(z) \gg \Im(z)$, the second is both the $\Re(z)$ and $\Im(z)$ are big real numbers of the same order and the last scenario is the $\Im(z)$ is big real number and $\Im(z) \gg \Re(z)$. Table 3.1 shows the computation of the $\check{\Gamma}_0(z)$ for large arguments.

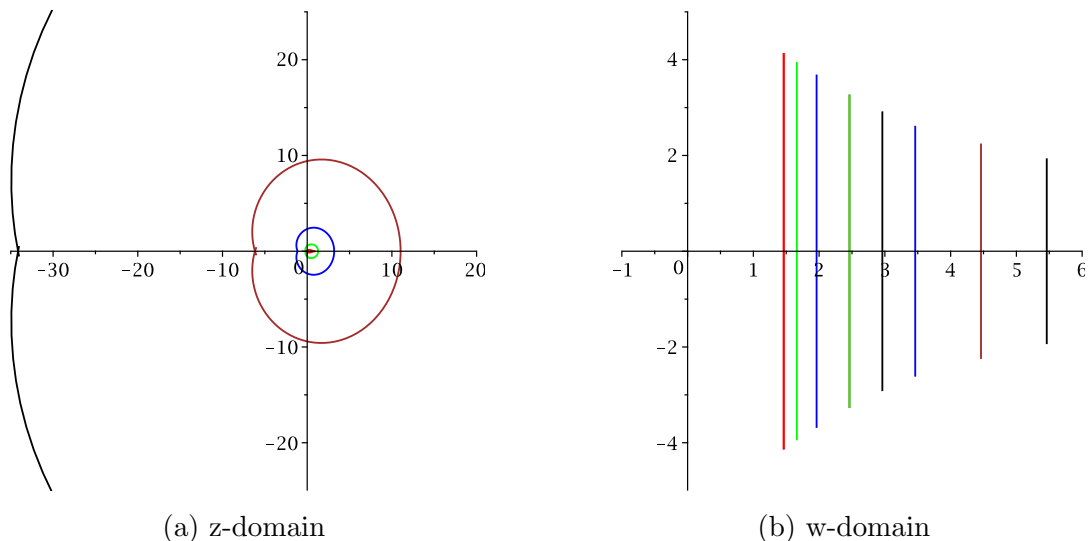


Figure 3.10: The range of the Principal branch of the Inverse function of $\Gamma(z)$ in the complex plane

z	$\check{\Gamma}_0(z)$
$10^{45000} + 10^{45}i$	$2309.20162 + 0.i$
$10^{450000} + 10^{450}i$	$98685.55560 + 0.i$
$10^{45000} + 10^{45000}i$	$12309.23842 + 0.08339.i$
$10^{450000} + 10^{450000}i$	$98685.58564 + 0.06829.i$
$10^{45} + 10^{45000}i$	$12309.20162 + 0.16678.i$
$10^{450} + 10^{450000}i$	$98685.55560 + 0.13659.i$

Table 3.1: Numerical computation of $\check{\Gamma}_0$ for larger arguments

And as we can see in the table 3.1, the contribution of the imaginary part of $\check{\Gamma}_0(z)$ becomes negligible for larger arguments z and $\check{\Gamma}_0(z) \rightarrow \Re(w)$.

When the contours shown in figure 3.8(b) are mapped using Γ into 3.8(a), they do not cover all points in the z -plane. It is necessary for the range to be in one-to-one correspondence with all of the domain, or else there will be values of z that have no $\check{\Gamma}_0(z)$. Therefore, we need to search for contours that fill in the drop-shaped region surrounding the origin in the z -plane, which is not yet filled. The required contours cannot start from the real axis, because the unused portion of the real axis has been assigned to other branches. This is a new feature of this function, relative to the log and arcsine functions above.

In constructing the contours shown in figure 3.11, we have to trim at both the lower end, which determines the right hand end of the drop shape, and the upper end which determines the left end. As we have seen, the values of $\check{\Gamma}_0$ tend to zero exponentially for large z , and so the contours crowd together at the origin. The trimming of the upper end of the contours therefore required a lot of magnification, but this is not shown, since the idea is shown already. When we combine the different sets of contours, we obtain figure 3.12. To complete the figure, it would be good to have expressions for the boundary of the region. Since the branch cut in the z -plane is along the negative real axis (and part of the positive real axis), we can easily say that the boundary is $\check{\Gamma}(-t)$ for $t > 0$. Then after one has written a program to evaluate complex values of $\check{\Gamma}$, we can plot the boundary. The plot, however, will be entirely numerical, and we prefer a closed-form approximate method. From Stirling's approximation, which was shown in figure 1.11 to be accurate in the complex plane, we have the approximation given above in (2.12) and repeated here for convenience.

$$\check{\Gamma} \sim \frac{1}{2} + \frac{\ln(z/\sqrt{2\pi})}{W_0(e^{-1} \ln(z/\sqrt{2\pi}))} .$$

Plotting this approximation for $z = -t$ and $t > 0$ gives the dotted curve added to figure 3.12. Finally, we have added numerical points on the boundaries to show how the region extends for values having negative real parts. The range of the principal branch clearly extends to negative infinity, but since it corresponds to arguments exponentially close to the origin, it does not need further detail.

Finally, we can ask what happens to the range as $z \rightarrow -\infty$ implying that $|\check{\Gamma}(z)| \rightarrow \infty$. Since we know that Lambert W has the asymptotic limit $W(z) \approx \ln z - \ln \ln z$, we can show that the range narrows, very slowly, so that the width parallel to the imaginary axis tends to zero.

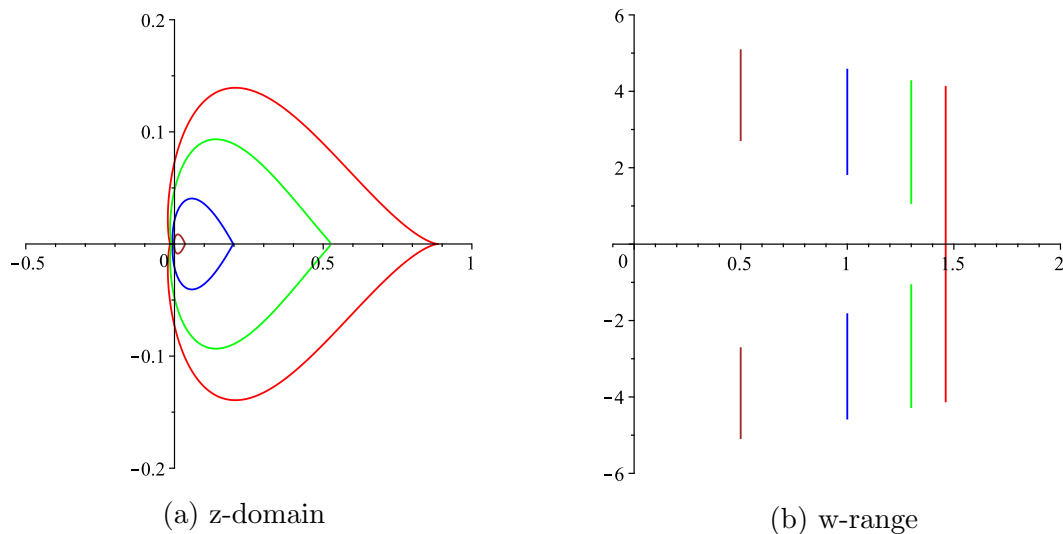


Figure 3.11: Extending the Principal branch of the inverse of $\Gamma(z)$ into the complex plane. Contours not starting from the real axis.

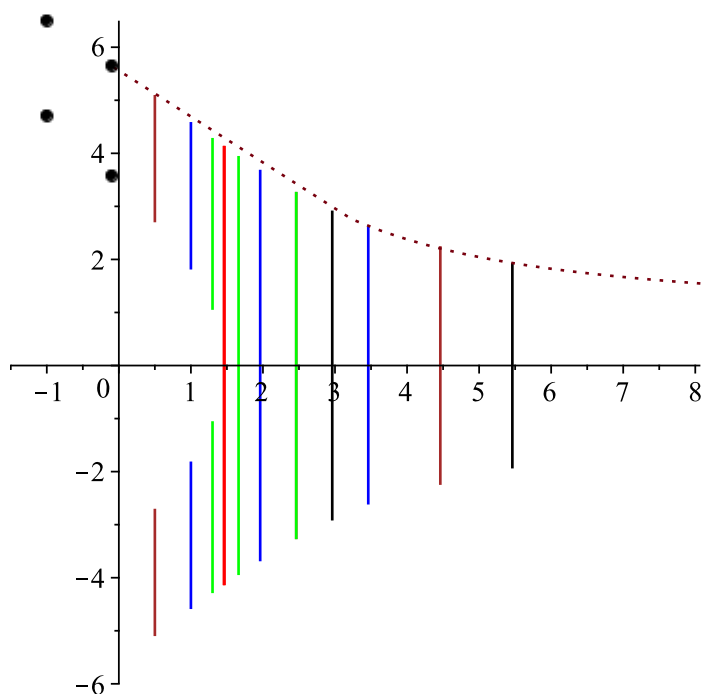


Figure 3.12: The range of the principal branch. The dotted line shows an approximation to the boundary. The large dots are points on the boundary showing how it extends for values with negative real part.

3.3.4 The extension of the other branches $\check{\Gamma}_k$ in complex plane

In this section, we shall repeat the process for other branches $\check{\Gamma}_k(z)$ starting with $\check{\Gamma}_{-1}(z)$.

The branch $\check{\Gamma}_{-1}(x)$ has two real domains and two associated ranges: the positive real

domain $[\gamma_0, \infty]$ and its positive range $[0, \psi_0]$, and the negative domain $]\infty, \gamma_{-1}]$ its negative range $]\psi_{-1}, 0[$. Following the same process, still using the map $w \mapsto \Gamma(w)$, figure 3.13 and 3.14 show the straight contours. The contours have already been trimmed so as to define

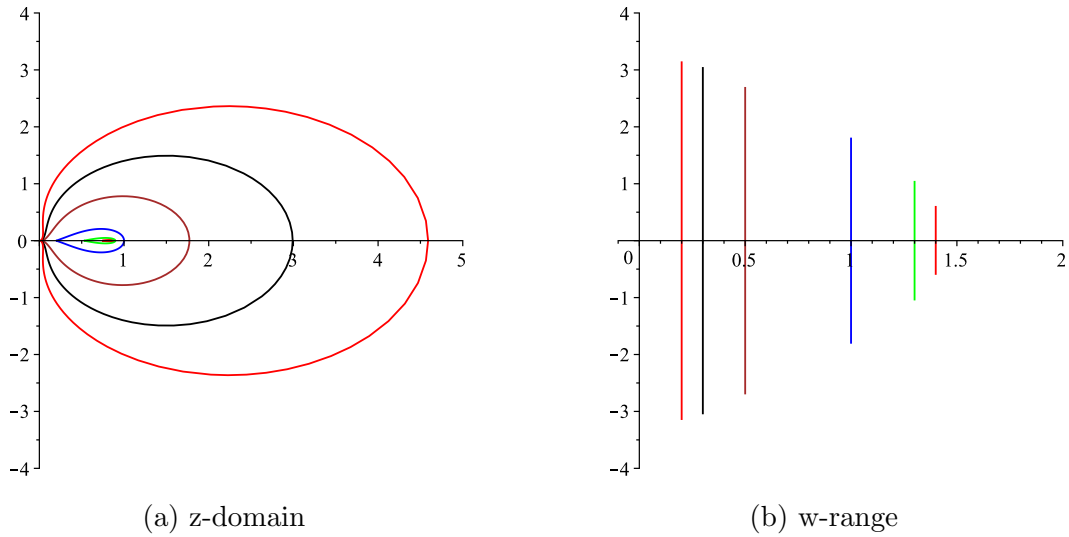


Figure 3.13: The extension of the positive $\check{\Gamma}_{-1}(x)$ into the complex plane

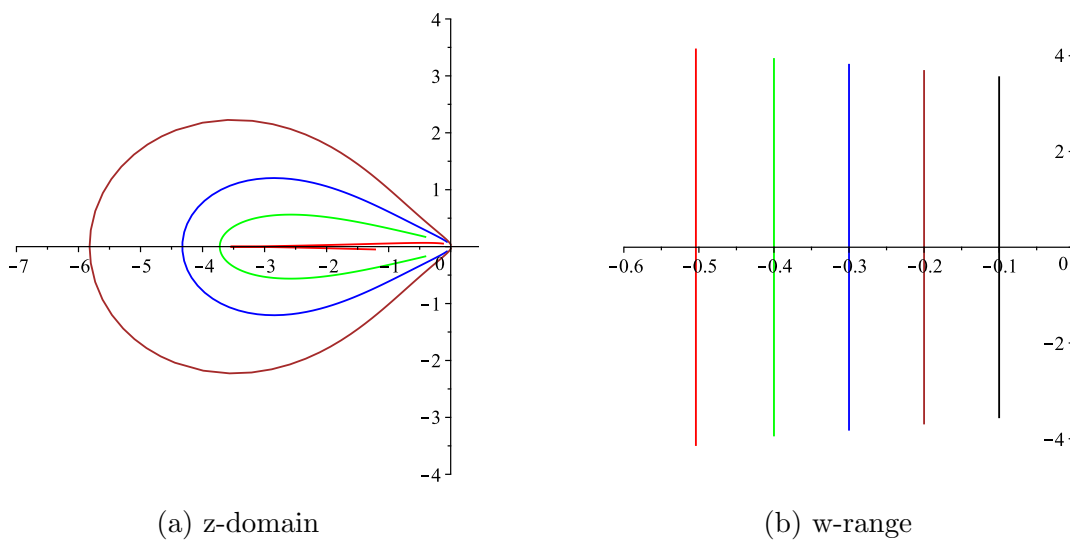


Figure 3.14: The extension of the negative $\check{\Gamma}_{-1}(x)$ into the complex plane

the range of the branch $k = -1$. As with the principal branch, there remains a small region which has not yet been filled during the mapping process. Again we must split the contours, because the remainder of the real line has been assigned to other branches.

The split contours and the remaining region are shown in figure 3.15. We now combine the various contours in figure 3.16. The process just described can be repeated for the

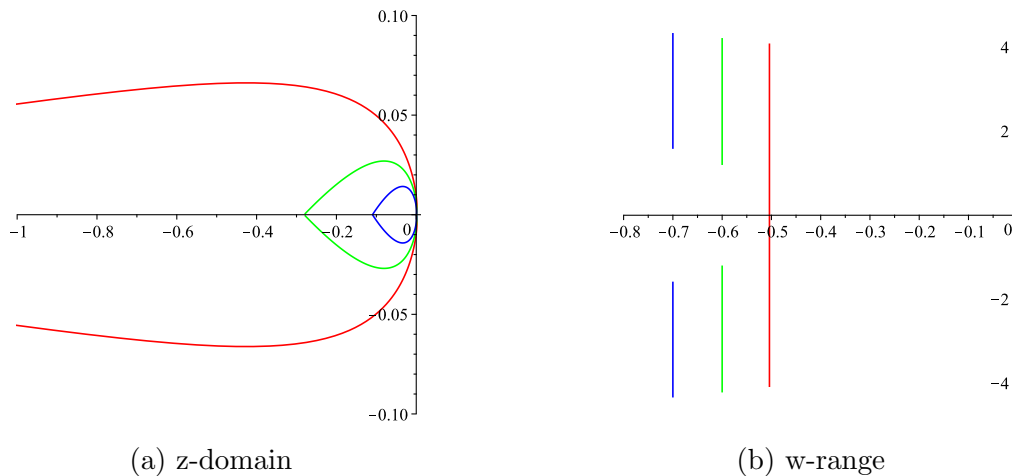


Figure 3.15: The extension of the positive $\check{\Gamma}_{-1}(x)$ into the complex plane

other branches. Since the principles are unchanged and the results are similar, we do not show more results explicitly. Instead we present a schematic illustration (an artistic impression) of the overall branch structure in figure 3.17. Note that the region outside the principal branch has not been studied, but we expect that branches with positive labels exist there.

3.4 Conclusion

In this chapter, we have used a contour technique to extend the $\check{\Gamma}_k$ in the complex plane. We only covered the principal branch $\check{\Gamma}_0$ and the positive domain of the branch $\check{\Gamma}_{-1}$ to set the motivation for a more rigorous approach for the other branches. New approximations formulas for $\check{\Gamma}_k$ should be proposed in the future. Finding more applications for the $\check{\Gamma}_k$ is the key to attract more interest from the research community. Other recent research interest is the extensions that are Stieltjes and Pick function and their integral representation. In [3], the author shows that the three holomorphic functions in

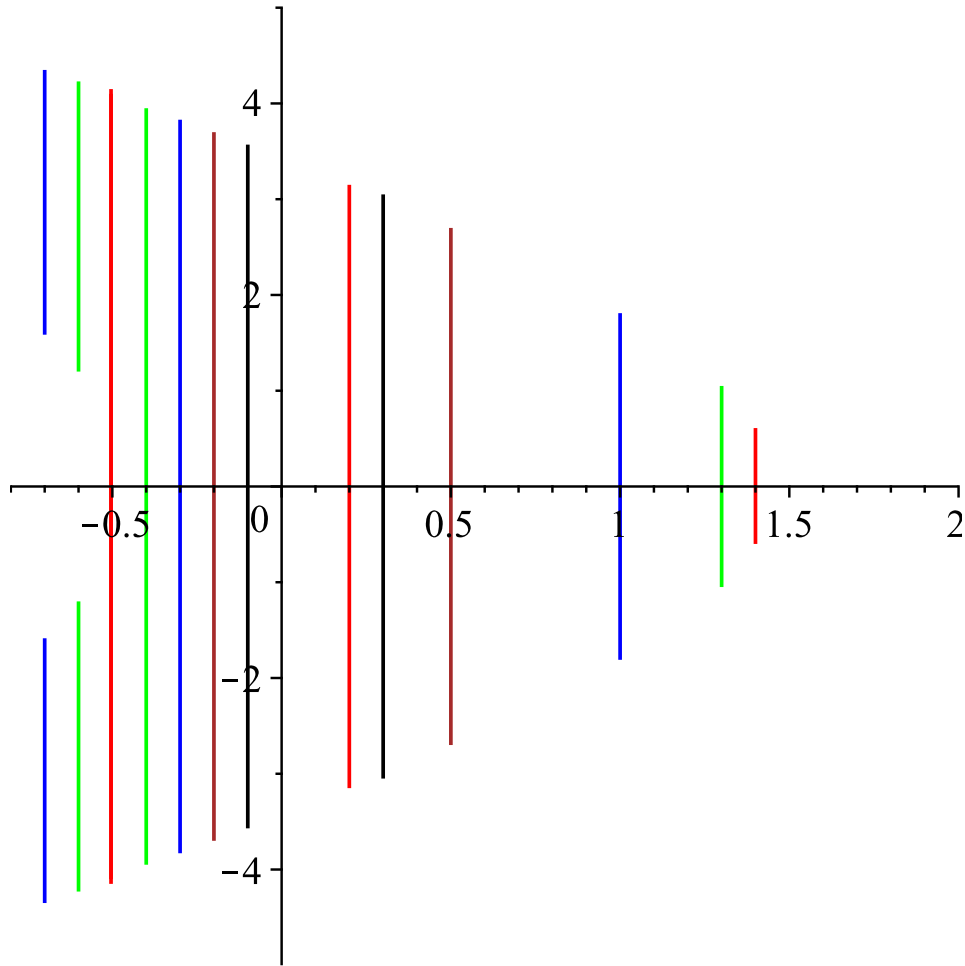


Figure 3.16: The range of the branch $\check{\Gamma}_{-1}$ in the complex plane.

$\mathbb{C} \setminus]-\infty, 0]$

$$\frac{\log \Gamma(z+1)}{z \operatorname{Log} z}$$

$$\frac{\log \Gamma(z+1)}{z}$$

$$z - \frac{\log \Gamma(z+1)}{\operatorname{Log} z}$$

are all Pick functions and found their integral representations. It will be interesting to find the integral representation of

$$\check{\Gamma}_0 \sim \frac{1}{2} + \frac{\log(z/\sqrt{2\pi})}{W_0(e^{-1} \log(z/\sqrt{2\pi}))} \quad z \in A$$

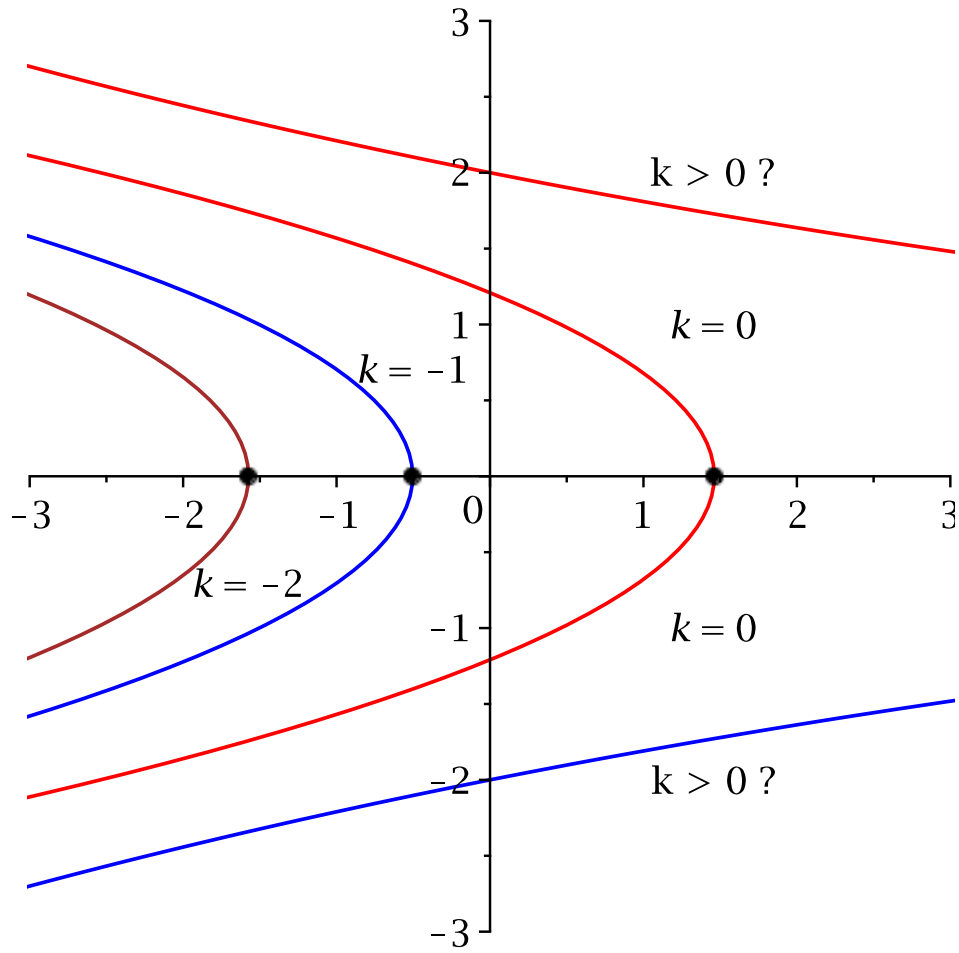


Figure 3.17: A schematic presentation of the ranges of the branches of $\tilde{\Gamma}_k$ in the complex plane, for $k \leq 0$.

where $A = \mathbb{C} \setminus]-\infty, e^{-1}\sqrt{2\pi}]$ and compare it with the numerical values of Newton's scheme result we got.

Bibliography

- [1] J. M. Borwein and R. M. Corless. The Gamma function in the Monthly. *American Mathematical Monthly*, 125(5):400–424, 2018.
- [2] H. L. Pedersen C. Berg. A completely monotone function related to the Gamma function. *J. Compt. and Appl. Math.*, 133(2001):219–230, 2000.
- [3] H. L. Pedersen C. Berg. Pick functions related to the Gamma function. *Journal of Mathematics*, 32(2), 2002.
- [4] S. L. Qiu C. D. Anderson. A monotoneity propriety of the Gamma function. *American Mathematical Society*, 125(11):3355–3362, 1997.
- [5] R. M. Corless and N. Fillion. *A Graduate Introduction to Numerical Methods: From the Viewpoint of Backward Error Analysis*. Springer New York, 2013.
- [6] T. Burić N. Elezović. New asymptotic expansions of the Gamma function and improvements of Stirling’s type formulas. *J. Comput. Anal. Appl.*, 13(4):785–795, 2011.
- [7] K. A. Folitse, D. J. Jeffrey, and R. M. Corless. Properties and computation of the functional inverse of Gamma. In J. Guerrero D. Zaharie, editor, *19th Symposium on Symbolic and Numeric Algorithms for Scientific Computing*, pages 1–5. IEEE computer soc., 2017.
- [8] G. H. Gonnet. Expected length of the longest probe sequence in hash code searching. *J. ACM*, 28(2), 1981.

- [9] C. Berg Horst Alzer. Some classes of completely monotonic functions. *Annales Academiae Scientiarum Fennicae*, 27(2001):445–460, 2002.
- [10] D. J. Jeffrey, D. E. G. Hare, and R. M. Corless. Unwinding the branches of the Lambert W function. *Math. Scientist*, 21:1–7, 1996.
- [11] David J. Jeffrey. Branch structure and implementation of Lambert W. *Mathematics in Computer Science*, 11(3-4):341–350, 2017.
- [12] C. Lanczos. A precision approximation of the Gamma function. *SINUM, Series B: Numerical Analysis*, 1(1):86–96, 1964.
- [13] D. F. Lawden. *Elliptic Functions and Applications*. Springer, 1989.
- [14] P. Luschny. Approximation formulas for the factorial function, 2003.
- [15] C. Mortici. An ultimate extremely accurate formula for approximations of the factorial function. *Arch. Math. (Basel)*, 93(1):37–45, 2009.
- [16] C. Mortici. A class of integral approximations for the factorial function. *Comput. Math. Appl.*, 59(6):2053–2058, 2010.
- [17] G. Nemes. New asymptotic expansions for the Gamma function. *Arch. Math. (Basel)*, 95(2):161–169, 2010.
- [18] G. Nemes. More accurate approximations for the Gamma function. *Thai. J Math.*, 9(1):21–28, 2011.
- [19] H. L. Pedersen. Inverses of Gamma functions. *Constructive Approximation*, 41(2):251–267, 2015.
- [20] G. R. Pugh. An analysis of the Lanczos Gamma approximation. *University of British Columbia*, 2004.

- [21] T. Schmelzer and L. N. Trefethen. Computing the Gamma function using contour integrals and rational approximations. *SIAM Journal on Numerical Analysis*, 45(2):558–571, 2007.
- [22] J. L. Spouge. Computation of the Gamma, digamma, and trigamma functions. *SIAM Journal on Numerical Analysis*, 31(3):931–944, 1994.
- [23] M. Uchiyama. The principal inverse of the Gamma function. *Proc. Amer. Math. Soc*, 140(4):1343–1348, 2012.
- [24] W. Wang. Unified approaches to the approximations of the Gamma function. *Journal of Number Theory*, 163:570–595, 2016.
- [25] E. Wegert. *Visual complex functions: An introduction with phase portraits*. Springer Science, 2012. Cambridge Books Online.
- [26] Gerald Wheatley. *Applied Numerical Analysis, Seventh Edition*. Addison-Wesley, 2004.

Curriculum Vitae

Name: Komla Amenyo Folitse

Post-Secondary Education and Degrees: University of Western Ontario
London, Ontario
2016 - 2018 M.Sc. Applied Mathematics

Related Work Experience: Research Assistant(Applied Mathematics)
University of Western Ontario
2016 - 2018

Teaching Assistant
University of Western Ontario
2016 - 2018